

Black strings in $(4 + 1)$ dimensional Einstein-Yang-Mills theory

Yves Brihaye

Faculte des Sciences, Universite de Mons-Hainaut, B-7000 Mons, Belgium

Betti Hartmann^y

School of Engineering and Science, International University Bremen, 28725 Bremen, Germany

Eugen Radu^z

Department of Mathematical Physics, National University of Ireland Maynooth, Ireland

March 27, 2022

Abstract

We study two classes of static uniform black string solutions in a $(4 + 1)$ -dimensional $SU(2)$ Einstein-Yang-Mills model. These configurations possess a regular event horizon and corresponds in a 4-dimensional picture to axially symmetric black hole solutions in an Einstein-Yang-Mills-Higgs-U(1)-dilaton theory. In this approach, one set of solutions possesses a nonzero magnetic charge, while the other solutions represent black holes located in between a monopole-antimonopole pair. A detailed analysis of the solutions' properties is presented, the domain of existence of the black strings being determined. New four-dimensional solutions are found by boosting the five-dimensional configurations. We also present an argument for the non-existence of finite mass hyperspherically symmetric black holes in $SU(2)$ Einstein-Yang-Mills theory.

1 Introduction

Black holes in more than four spacetime dimensions have a much richer spectrum of horizon topologies than their four-dimensional counterparts. In a d -dimensional asymptotically flat spacetime, the static vacuum black hole of a certain mass with horizon topology S^{d-2} is uniquely described by the Schwarzschild-Tangherlini solution [1]. While this solution is hyperspherically symmetric, so-called black strings also exist [2]. Such configurations are important if one supposes the existence of extra dimensions in the universe, which are likely to be compact and described by a Kaluza-Klein (KK) theory. The simplest vacuum static solution of this type (and the only one known in closed form) is found by assuming translational symmetry along the extra coordinate direction and corresponds to a uniform black string with horizon topology $S^{d-3} \times S$. Though this solution exists for all values of the mass, it is unstable below a critical value as shown by Gregory and Laamane [3]. This was interpreted to mean that a light uniform string decays to a (hyperspherical) black hole since that has higher entropy. However, Horowitz and Maeda [4] argued that such a transition has an intermediate step: the light uniform string decays to a non-uniform string, which then eventually decays to a black hole. This prompted a search for this missing link, and a branch of non-uniform black string solutions was found in [5, 6]. Nevertheless, a number of aspects still remain to be clarified and the literature on non-uniform black string solutions is continuously growing (see [7] for a recent review).

yves.brihaye@umh.ac.be

^yb.hartmann@iu-bremen.de

^zradu@thphys.nuim.ie

The uniform black string solutions have been explored from many points of view, in particular by including various matter fields. However, most of the studies in the literature restricted to the case of an abelian matter content. At the same time, a number of results obtained in the literature clearly indicates that the solutions of Einstein's equations coupled to nonabelian matter fields possess a much richer structure than in the $U(1)$ case (see [8] for a survey of the situation in $d = 4$). Here the only case systematically discussed in the literature is $d = 5$ and an $SU(2)$ gauge field, for an ansatz with no dependence on the extra z coordinate. No exact solutions with reasonable asymptotics are available analytically in this case and the field equations have to be solved numerically. As a new feature, both globally regular and black string solutions are possible to exist. The simplest vortex-type configurations have been constructed in [9] and are spherically symmetric in four dimensions, extending trivially into one extra dimension. The black string counterparts of these solutions have been constructed recently in [10] and found to present a complicated branch structure.

However, as argued in [11], the existence of a nonabelian winding number implies a very rich set of possible boundary conditions, the configurations which are spherically symmetric in four dimensions corresponding to the simplest case. A discussion of a more general set of vortex-type, globally regular solutions have been presented in [11]. In a four dimensional picture these correspond to axially symmetric multimonopoles (MM), respectively monopole-antimonopole (MA) solutions in an Einstein-Yang-Mills-Higgs (EYMH) theory with a non-trivial coupling to a Maxwell and a dilaton field. A preliminary discussion of the black string counterparts of some of these solutions has been presented in [12].

It is the purpose of this paper to present a systematic analysis of the uniform black string solutions in Einstein-Yang-Mills (EYM) theory in five spacetime dimensions, for two different sets of boundary conditions satisfied by the matter fields at infinity. Apart from the solutions discussed in [10], we present a detailed study of the deformed black string configuration, which in the $(3+1)$ -dimensional reduced theory can be interpreted as describing axially symmetric multimonopole black holes, respectively nonabelian black holes with magnetic dipole hair. Although all fields are independent on the extra coordinate, the event horizon of these solutions is deformed (the horizon circumference along the equator differs from the corresponding quantity evaluated along the poles), which resembles the non-uniform black string case [5, 6].

Although the no hair conjecture is known to be violated for $d = 5$ solutions with one compact extra dimension (see e.g. the discussion in [13]) the solutions presented in this paper provide another counterexample to this conjecture. However, this is not a surprise, given the relation noticed above with the $(3+1)$ -dimensional theory, which is known to present hairy black hole solutions.

As already noticed in [12], after boosting the $d = 5$ configurations and reducing to $d = 4$, we obtain new four dimensional solutions which rotate and present a nonzero nonabelian electric charge. For the particular case of configurations which are spherically symmetric in four dimensions, this procedure generates $d = 4$ dyonic black holes.

We argue here that these solutions are interesting from yet another point of view. Different from other known theories, no $d = 5$ hyperspherically symmetric nitemass EYM solutions exist in five dimensions, unless one considers the inclusion of higher order curvature terms in the action [14]. The nonexistence proof for the globally regular case has been presented in [9] (see also [15]). In Appendix A, we present a similar argument for black hole solutions. Therefore, the simplest $d = 5$ solutions of the EYM theory corresponds to uniform vortices and black strings.

Our paper is organized as follows: In Section 2, we give the model including the Ansatz and the boundary conditions. In Section 3, we describe our numerical results. The properties of the vortex solutions are also reviewed, a number of new results being presented. In Section 4, we comment on the new $d = 4$ solutions that we obtain by boosting the $d = 5$ EYM configurations and in Section 5 we give our conclusions.

Most of the notations and sign conventions used in this paper are similar to those in Ref. [11].

2 The model

2.1 Action principle

We consider the five dimensional SU(2) Einstein-Yang-Mills (EYM) action

$$I_5 = \int d^5x \sqrt{-g_5} \left[-\frac{R}{16G} - \frac{1}{2g^2} \text{Tr} F_{MN} F^{MN} \right] \quad (1)$$

(throughout this paper, the indices M, N, \dots will denote the five dimensional coordinates and μ, ν, \dots the coordinates of the four dimensional physical spacetime).

Here G is the gravitational constant, R is the Ricci scalar associated with the spacetime metric g_{MN} and $F_{MN} = \frac{1}{2} f_{MN}^{(a)} A_M^{(a)} A_N^{(a)}$ is the gauge field strength tensor defined as $F_{MN} = \partial_M A_N - \partial_N A_M + i[A_M, A_N]$; where the gauge field is $A_M = \frac{1}{2} A_M^{(a)} T^a$; T^a being the Pauli matrices and g the gauge coupling constant.

Variation of the action (1) with respect to g^{MN} and A_M leads to the field equations

$$R_{MN} - \frac{1}{2} g_{MN} R = 8G T_{MN}; \quad (2)$$

$$D_M F^{MN} + i[A_M, F^{MN}] = 0; \quad (3)$$

where the YM stress-energy tensor is

$$T_{MN} = 2 \text{Tr} (F_{MP} F_{NQ} g^{PQ} - \frac{1}{4} g_{MN} F_{PQ} F^{PQ}); \quad (4)$$

2.2 The ansatz

In what follows we will consider uniform black string configurations, assuming that both the matter functions and the metric functions are independent on the extra coordinate $x^5 = z$. Without any loss of generality, we consider a five dimensional metric parametrization

$$ds^2 = e^{-a} (dx^2 + dy^2 + dz^2 + 2W dx^2); \quad (5)$$

with $a = 2\sqrt{\frac{2}{3}}$.

The four dimensional reduction of this theory with respect to the Killing vector ∂_z has been presented in [11]. For the reduction of the YM action term, a convenient SU(2) ansatz is

$$A = A dx^2 + g (dz + 2W dx^2); \quad (6)$$

where W is a U(1) potential, A is a purely four dimensional gauge field potential, while g corresponds after the dimensional reduction to a triplet Higgs field.

This leads to the four dimensional action principle

$$I_4 = \int d^4x \sqrt{-g_4} \left[-\frac{1}{4G} R - \frac{1}{2} \text{Tr} F_{\mu\nu} F^{\mu\nu} - \frac{1}{2} (D_\mu g)^2 - \frac{1}{4} G^2 \right] \quad (7)$$

where R is the Ricci scalar for the metric $g_{\mu\nu}$, while $F_{\mu\nu} = \partial_\mu A_\nu - \partial_\nu A_\mu + i[A_\mu, A_\nu]$ and $G = \partial_\mu W - \partial_\nu W$ are the SU(2) and U(1) field strength tensors defined in $d=4$.

Here we consider five dimensional configurations possessing two more Killing vectors apart from ∂_z . These are $\partial_t = \partial_{x^0}$, corresponding to an axial symmetry of the four dimensional metric sector (where the azimuthal angle ϕ ranges from 0 to 2π), and $\partial_\tau = \partial_{x^1}$, with τ the time coordinate.

We consider the following parametrization of the four dimensional line element, employed also to find globally regular solutions

$$d^2s = -dt^2 - d\tau^2 = -f(r) dt^2 + \frac{q(r)}{f(r)} (dr^2 + r^2 d\phi^2) + \frac{l(r)}{f(r)} r^2 \sin^2 \theta d\theta^2; \quad (8)$$

and the function g_{zz} depending also on r ; only. Here t is the time coordinate, r is the radial coordinate while $0 < \theta < \pi$ is a polar angle.

We take the event horizon to reside at a surface of constant radial coordinate $r = r_h > 0$, characterized by the condition $f(r_h) = 0$, i.e: $g_{tt} = 0$. The remaining metric potentials take nonzero and finite values at the event horizon.

The construction of the corresponding YM ansatz compatible with the spacetime symmetries has been discussed in [11]. For the time and extra-direction translational symmetry, we choose a gauge such that $\partial A = \partial t = \partial A = \partial z = 0$. However, the action of the Killing vector ∂_t can be compensated by a gauge rotation $L \cdot A_N = D_N$; with L being a Lie-algebra valued gauge function [16]. According to the standard analysis, this introduces a winding number n in the ansatz (which is a constant of motion and is restricted to be an integer).

As discussed in [11], the most general 5d dimensional Yang-Mills ansatz compatible with these symmetries contains 15 functions: 12 magnetic and 3 electric potentials

$$A_N = \frac{1}{2} A_N^{(r)}(r; \theta) \frac{n}{r} + \frac{1}{2} A_N^{(\theta)}(r; \theta) + \frac{1}{2} A_N^{(\phi)}(r; \theta) \frac{n}{r}; \quad (9)$$

where $\frac{n}{r}$, $\frac{n}{r}$ and $\frac{n}{r}$ denote the scalar product of the vector of Pauli matrices $\vec{\sigma} = (\sigma_1; \sigma_2; \sigma_3)$ with the unit vectors $\vec{e}_r^n = (\sin \theta \cos n'; \sin \theta \sin n'; \cos \theta)$, $\vec{e}_\theta^n = (\cos \theta \cos n'; \cos \theta \sin n'; \sin \theta)$, $\vec{e}_\phi^n = (\sin n'; \cos n'; 0)$.

Searching for solutions within the most general ansatz is a difficult task. Therefore, similar to [11] we use a purely magnetic reduced ansatz with six essential nonabelian potentials and

$$A_r^{(r)} = A_r^{(\theta)} = A_r^{(\phi)} = A_r^{(\phi)} = A_r^{(\phi)} = A_5^{(\phi)} = A_t^{(a)} = 0:$$

The consistency of this reduction has been verified at the level of the YM equations.

However, for configurations with a nontrivial θ -dependence the gauge potentials A_r ; A_5 have components along the same directions in isospace, which implies that the T_{55} component of the energy-momentum tensor will be nonzero [11]. Thus the Einstein equations imply the existence, in the 5d dimensional metric ansatz (5), of one extradiagonal $g_{5\theta}$ metric function, i.e:

$$W = J(r; \theta) \theta': \quad (10)$$

A suitable parametrization of the nonzero components of $A_N^{(a)}$ which factorizes the trivial θ -dependence and admits a straightforward four dimensional picture is:

$$\begin{aligned} A_r^{(\phi)} &= \frac{1}{r} H_1(r; \theta); \quad A_r^{(\theta)} = 1 - H_2(r; \theta); \quad A_r^{(r)} = n \sin \theta H_3(r; \theta) + 2gJ(r; \theta) \frac{1}{r}; \\ A_r^{(\phi)} &= n \sin \theta (1 - H_4(r; \theta)) + 2gJ(r; \theta) \frac{2}{r}; \quad A_5^{(r)} = \frac{1}{r} H_1(r; \theta); \quad A_5^{(\theta)} = \frac{2}{r} H_2(r; \theta); \end{aligned} \quad (11)$$

The gauge invariant quantities expressed in terms of these functions will be independent on the angle θ .

To fix the residual abelian gauge invariance we choose the gauge condition

$$r \partial_r H_1 - \partial_\theta H_2 = 0:$$

The $d = 5$ EYM configurations extremize also the action principle (7) and can be viewed as solutions of the four dimensional theory. In this picture, $H_1(r; \theta)$ are the magnetic SU(2) gauge potentials, $\theta(r; \theta)$ is a dilaton, $J(r; \theta)$ is a U(1) magnetic potential, while $\frac{1}{r} H_3(r; \theta)$; $\frac{2}{r} H_2(r; \theta)$ are the components of a Higgs field. We mention also that, similar to the pure (E)-YM H case, one may define a 't Hooft field strength tensor and an expression for the nonabelian electric and magnetic charges within the action principle (7).

2.3 Particular solutions

Restricting to configurations which are spherically symmetric in $d = 4$, one exact solution of the $d = 5$ EYM equations is found taking the product of the $d = 4$ Schwarzschild black hole with a circle (here we consider an isotropic coordinate system)

$$ds^2 = \left(1 + \frac{r_h}{2r}\right)^4 dr^2 + r^2 d\Omega^2 - \frac{1}{1 + \frac{r_h}{2r}} dt^2 + dz^2; \quad (12)$$

and for a pure gauge $SU(2)$ field $H_1 = H_3 = \alpha_2 = 0$, $\alpha_1 = \text{const}$; $H_2 = H_4 = 1$, the event horizon being located at $r = r_h = 2 > 0$.

The second solution is more important and corresponds to an embedded $U(1)$ configuration with

$$ds^2 = \frac{r^2 + 2(r_+ + r_-)r + (r_+ - r_-)^2}{4r^2} dr^2 + r^2 d\tau^2 - \frac{1}{r^2 + 2(r_+ + r_-)r + (r_+ - r_-)^2} dt^2 + \frac{1}{r^2 + 2(r_+ + r_-)r + (r_+ - r_-)^2} dz^2; \quad (13)$$

and $H_i = \alpha_2 = 0$, $\alpha_1 = \text{const}$; where r_+ and r_- are two constants with $r_+ r_- = 4^{-2} n^2 = 3$. In a four dimensional perspective, this describes a Dirac monopole in an Einstein-Maxwell-dilaton theory (the $U(1)$ field originating here from the $d = 5$ nonabelian field), with a dilaton coupling constant $1 = \frac{1}{3}$ (see e.g. [17]). These solutions have a regular event horizon at $r = r_+ - r_-$. There is also a curvature singularity at $r = r_-$. The physical mass of the solution is $M = (2r_+ + r_-) = 4$, while the magnetic charge is $Q_M = \frac{1}{3r_+ r_-} = 2$.

2.4 Boundary conditions

2.4.1 Metric functions

To obtain finite energy density black string solutions that asymptote to $M^4 \times S^1$, where M^4 is the four dimensional Minkowski spacetime, the metric functions have to satisfy the boundary conditions

$$\partial_r f|_{r=r_h} = f'|_{r=r_h} = q'|_{r=r_h} = l'|_{r=r_h} = \partial_r J|_{r=r_h} = 0; \quad (14)$$

on the event horizon, and

$$f|_{r=1} = q|_{r=1} = l|_{r=1} = 1; \quad j|_{r=1} = J|_{r=1} = 0; \quad (15)$$

at infinity. For solutions with parity reflection symmetry (the case considered in this paper), the boundary conditions along the z and θ axes are (with $z = r \cos \theta$ and $\theta = r \sin \theta$)

$$\partial_\theta f|_{\theta=0; \theta=\pi} = \partial_\theta J|_{\theta=0; \theta=\pi} = \partial_\theta f|_{\theta=0; \theta=\pi} = \partial_\theta q|_{\theta=0; \theta=\pi} = \partial_\theta l|_{\theta=0; \theta=\pi} = 0; \quad (16)$$

2.4.2 Matter functions

In [11] the following general set of boundary conditions at $r \rightarrow 1$ has been proposed for the magnetic potentials α_1 and α_2

$$\lim_{r \rightarrow 1} \alpha_1 = \cos m; \quad \lim_{r \rightarrow 1} \alpha_2 = \sin m; \quad (17)$$

with $m = 0, 1, \dots$, and α an arbitrary constant.

The expression of the boundary conditions satisfied by the gauge functions H_i at $r \rightarrow 1$ depends on the value of m and is given in [11]. In this paper we restrict ourselves to the simplest cases, $m = 0$ and $m = 1$, corresponding in a four dimensional picture to multimonopoles (MM) and monopole-antimonopole (MA) configurations, respectively. For $m = 0$ one finds

$$H_i|_{r=1} = 0; \quad (18)$$

with $i = 1, 4$, while the $m = 1$ solutions are found within a set of boundary conditions

$$H_1|_{r=1} = H_2|_{r=1} = 0; \quad H_3|_{r=1} = H_4|_{r=1} = 1; \quad (19)$$

In both cases, the boundary values at the event horizon are

$$H_1|_{r=r_h} = 0; \quad \partial_r H_2|_{r=r_h} = \partial_r H_3|_{r=r_h} = \partial_r H_4|_{r=r_h} = 0; \quad \partial_r \alpha_1|_{r=r_h} = \partial_r \alpha_2|_{r=r_h} = 0; \quad (20)$$

The conditions along the axes are determined by the symmetries and finite energy density requirements. For $m = 0$ solutions we impose

$$H_{1j=0; \pm 2} = H_{3j=0; \pm 2} = \partial_{\pm 2} j = 0; \partial_{\pm 2} H_{2j=0; \pm 2} = \partial_{\pm 2} H_{4j=0; \pm 2} = \partial_{\pm 1} j = 0; \pm 2 = 0; \quad (21)$$

which in a four-dimensional picture implies a magnetic charge $Q_M = n$. The conditions satisfied by the $m = 1$ configurations are

$$\begin{aligned} H_{1j=0; \pm 2} = H_{3j=0; \pm 2} = \partial_{\pm 2} H_{2j=0; \pm 2} = \partial_{\pm 2} H_{4j=0; \pm 2} = 0; \\ \partial_{\pm 1} j = 0 = \partial_{\pm 1} j = \pm 2 = \partial_{\pm 2} j = 0 = \partial_{\pm 2} j = \pm 2 = 0; \end{aligned} \quad (22)$$

In addition, regularity on the z axis requires the conditions $lj = 0 = qj = 0, H_{2j=0} = H_{4j=0}$ to be satisfied, for any values of the integers $(m; n)$.

2.5 Physical parameters

The physical parameters of the solution can be computed by taking either a five-dimensional viewpoint, or in terms of the four-dimensional theory that is obtained via KK reduction. Both kind of viewpoints are of course directly related, but the five-dimensional theory is simpler and so we take this viewpoint in this section.

For a given solution we consider the asymptotic region as defined by $r \rightarrow 1$. The field equations imply the following asymptotic form of the relevant metric potentials g_{tt} and g_{zz}

$$g_{tt} \sim 1 + \frac{c_t}{r} + O(1/r^2); \quad g_{zz} \sim 1 + \frac{c_z}{r} + O(1/r^2); \quad (23)$$

while the functions which enter the four-dimensional line element (8) behave for large r as

$$f \sim 1 + \frac{f_1}{r} + O(1/r^3); \quad q \sim 1 + \frac{q_1 + q_2 \sin^2}{r^2} + O(1/r^3); \quad l \sim 1 + \frac{q_1}{r^2} + O(1/r^3); \quad (24)$$

where c_t, c_z, f_1, q_1 and q_2 are arbitrary real constants (with $f_1 = c_z = 2 - c_t$).

Here it is convenient to use the general formalism proposed in [18] (see also [19]). The $d = 5$ spacetime has a translation-invariant direction z and hence it can be assigned a 2×2 ADM stress-energy tensor $T_{ab}, a; b = t; z$. This is computed from the asymptotic metric $g_{MN} = g_{MN}^h + h_{MN}$ (in Cartesian coordinates) as

$$T_{ab} = \frac{1}{16\pi G} \int_{(2)} d^2 n^i \left[\partial_i h_c^c + \partial_i h_j^j - \partial_j h_i^j - \partial_i h_{ab} \right] \quad (25)$$

where n^i is the radial normal vector and $a; b; c$ run over parallel directions $t; z$ while $i; j$ run over transverse directions. The integration is over the transverse angular directions. Using this we obtain the mass and momentum as the integrated energy and momentum densities.

In terms of c_t, c_z the mass M and the tension \sim along the z -direction are given by

$$M = \frac{L}{4G} [2c_t - c_z]; \quad \sim = \frac{1}{4G} [c_t - 2c_z]; \quad (26)$$

where L is the length of the extra dimension, which – if not stated differently – is set to one in this paper. Note that a similar mass expression is found by applying the Hawking-Horowitz mass formula [20]. Another relevant quantity here is the relative tension [21] defined as

$$n_t = \frac{\sim L}{M} = \frac{c_t - 2c_z}{2c_t - c_z}; \quad (27)$$

with $0 \leq n_t \leq 2$ for any $d = 5$ static solution. A vacuum uniform black string has $n_t = 1/2$ and exists for all values of M , while in the nonuniform case, knowing the exact curve of a branch in the $(M; n_t)$ phase diagram enables one to obtain the entire thermodynamics of that branch.

2.6 Temperature, entropy and deformation of the horizon

The zeroth law of black hole physics states that the surface gravity is constant at the horizon of the black hole solutions, where

$$\kappa^2 = -(1/4)g^{tt}g^{ij}(\partial_i g_{tt})(\partial_j g_{tt}) \Big|_{r=r_h} : \quad (28)$$

To evaluate κ , we use the following expansions of the metric functions at the horizon

$$\begin{aligned} f(r; \alpha) &= f_2(\alpha) \frac{r - r_h}{r_h}^2 + O\left(\frac{r - r_h}{r_h}^3\right); \\ q(r; \alpha) &= q_2(\alpha) \frac{r - r_h}{r_h}^2 + O\left(\frac{r - r_h}{r_h}^3\right); \\ l(r; \alpha) &= l_2(\alpha) \frac{r - r_h}{r_h}^2 + O\left(\frac{r - r_h}{r_h}^3\right); \end{aligned} \quad (29)$$

Since from general arguments the Hawking temperature T is proportional to the surface gravity, $T = \kappa/(2\pi)$; we obtain the relation

$$T = \frac{f_2(\alpha)}{2\pi r_h q_2(\alpha)} : \quad (30)$$

One can show, with help of the (r, θ) Einstein equation which implies

$$f_2 q_{2,\alpha} = 2 q_2 f_{2,\alpha}; \quad (31)$$

that the temperature T , as given in (30), is indeed constant.

For the line element (8), the area A of the event horizon is given by

$$A = 2L \int_0^Z d\theta \sin \theta \frac{p \sqrt{l_2(\alpha) q_2(\alpha)}}{f_2(\alpha)} r_h^2 : \quad (32)$$

According to the usual thermodynamic arguments, the entropy S is proportional to the area A

$$S = \frac{A}{4G}; \quad (33)$$

leading to the product

$$TS = \frac{r_h L}{4G} \int_0^Z d\theta \sin \theta \frac{p \sqrt{l_2(\alpha)}}{f_2(\alpha)} : \quad (34)$$

The horizon parameter r_h entering the boundary conditions is not a physical parameter. We thus introduce the area parameter x with

$$x = \frac{r_h}{4L} \frac{A}{L} \quad (35)$$

to characterize the solutions.

Since the energy density of the matter fields is angle dependent at the horizon, the horizon will be deformed. A suitable parameter to measure the deformation of the horizon of the black string solutions is given by the ratio $\beta = L_e/L_p$ of the horizon circumference along the equator

$$L_e = \int_0^{2\pi} d\theta' e^{a/2} \frac{1}{f} \sin \theta' r^A \Big|_{r=r_h} = 2\pi r_h; \quad \beta = 2 \quad (36)$$

and along the poles

$$L_p = 2 \int_0^Z d\theta e^{a/2} \frac{r}{f} \frac{q}{r^A} \Big|_{r=r_h, \theta'=0} : \quad (37)$$

Note that the non-uniform black string solutions [5, 6] have also a deformed horizon, with a different physical origin, however.

2.7 A computation of the Euclidean action

The expression (33) for the entropy can be derived in a more rigorous way by using Euclidean quantum gravity arguments. Here we start by constructing the path integral [22]

$$Z = \int \mathcal{D}g \mathcal{D}\phi e^{-i \int \mathcal{L} g; \phi} \quad (38)$$

by integrating over all metric and matter fields between some given initial and final hypersurfaces, corresponding here to the $SU(2)$ potentials. By analytically continuing the time coordinate $t \rightarrow i\tau$, the path integral formally converges, and in the leading order one obtains

$$Z \approx e^{-I_{cl}} \quad (39)$$

where I_{cl} is the classical action evaluated on the equations of motion of the gravity/matter system. In computing I_{cl} , one should supplement (1) with the boundary term

$$I_b = \frac{1}{8\pi G} \int_{\partial M} d^4x \sqrt{h} (K - K_0); \quad (40)$$

where K is the trace of the extrinsic curvature for the boundary ∂M and h is the induced metric of the boundary. In (40) we have already subtracted the contribution of the background spacetime which is taken to be flat space $M^4 \rightarrow S^1$.

We note that the considered Lorentzian solutions of the EYM equations extremize also the Euclidean action, $t \rightarrow i\tau$ having no effects at the level of the equations of motion. The value of β is found here by demanding regularity of the Euclideanized manifold as $r \rightarrow r_h$, which together with the expansion (29) gives $\beta = 1/T$. The physical interpretation of this formalism is that the class of regular stationary metrics forms an ensemble of thermodynamic systems at equilibrium temperature T [23]. Z has the interpretation of the partition function and we can define the free energy of the system $F = -\log Z$. Therefore

$$\log Z = -F = S - M; \quad (41)$$

or

$$S = M - I_{cl}; \quad (42)$$

straightforwardly follows.

To compute I_{cl} , we make use of the Einstein equations, replacing the Ricci volume term with $2R_t^t = 16\pi G T_t^t$. For our purely magnetic ansatz, the term T_t^t exactly cancels the matter field lagrangian in the bulk action $L_m = -\frac{1}{2}g^2 \text{Tr}(F_{MN} F^{MN})$ (see also the general discussion in [24]). The divergent contribution given by the surface integral term at infinity in R_t^t is canceled by the boundary action (40) and we arrive at the simple finite expression

$$I_{cl} = (2\alpha_t - \alpha_z) \frac{L}{4\pi G} - \frac{L}{2G} \int_0^Z d\sin \frac{\sqrt{\frac{f_2(\phi) - f_2(\phi_h)}{f_2(\phi)}}}{f_2(\phi)} r_h^2 \quad (43)$$

Replacing now in (42) (where M is the mass-energy computed in Section 2.4), we find

$$S = \frac{L}{2G} \int_0^Z d\sin \frac{\sqrt{\frac{f_2(\phi) - f_2(\phi_h)}{f_2(\phi)}}}{f_2(\phi)} r_h^2; \quad (44)$$

which is one quarter of the event horizon area, as expected.

3 Numerical solutions

For a nonvanishing magnitude of the gauge potential A_5 at infinity, it is convenient to work with dimensionless variables by taking the rescalings $r \rightarrow r/g$ and $t \rightarrow t/g$. Thus the field equations depend only on the coupling constants $\kappa = \frac{1}{4G}$, yielding the dimensionless mass (per unit length of the extra dimension) $m = (4G)^{-1}M$, the dimensionless tension being $\mu = (4G)^{-1}\tilde{\mu}$. For $\mu = 0$ (no gravity) and no dependence on the z -coordinate, the four dimensional picture corresponds to the $SU(2)$ -YM H theory in a flat M^4 background.

The solutions' properties crucially depend on the value of m and will be discussed separately for $m = 0$ and $m = 1$. In each case, we start by presenting a review of the globally regular vortex-type configurations which turn out to be crucial in the understanding of the domain of existence of the uniform black string solutions.

The spherically symmetric solutions are found by using the differential equation solver COLSYS [25]. In the axially symmetric case, the resulting set of eleven partial differential equations are solved by using the program FIDISO L, based on the iterative Newton-Raphson method. Details of the FIDISO L code are presented in [26]. In this scheme, a new radial variable is introduced which maps the semi infinite region $[r_h; \infty)$ to the closed region $[0; 1]$. Our choice for this transformation was $x = 1 - r_h/r$. Typical grids have sizes 100×30 , covering the integration region $0 \leq x \leq 1$ and $0 \leq t \leq 2$. The typical numerical error for the functions is estimated to be on the order of 10^{-3} .

3.1 $m = 0$ vortex-type configurations

The equations of motion admit next to black string solutions also vortex-type solutions which exist on the full interval $[0; 1]$. The boundary conditions satisfied by these solutions as $r \rightarrow \infty$ and on the axes are similar to the black string case, while as $r \rightarrow 0$ one imposes

$$\begin{aligned} H_1|_{j=0} = H_3|_{j=0} = 0; H_2|_{j=0} = H_4|_{j=0} = 1; \quad \dot{\alpha}|_{j=0} = \dot{\beta}|_{j=0} = 0; \\ \partial_r f|_{j=0} = \partial_r q|_{j=0} = \partial_r l|_{j=0} = J|_{j=0} = 0; \end{aligned} \quad (45)$$

3.1.1 Spherically symmetric solutions

For $m = 0$; $n = 1$, all metric and matter functions depend only on the radial coordinate r . For the matter functions we then have

$$H_1 = H_3 = \dot{\alpha} = \dot{\beta} = 0; H_2 = H_4 = K(r); \quad \alpha = \beta(r); \quad (46)$$

while for the metric functions we get $J = 0$ and $q = 1$ such that the metric becomes diagonal:

$$ds^2 = e^{-a(r)} \left(-f(r) dt^2 + \frac{q(r)}{f(r)} dr^2 + r^2 d\Omega^2 + r^2 \sin^2 \theta d\varphi^2 \right) + e^{2a(r)} dz^2; \quad (47)$$

In [9] it has been found that several branches of solutions can be constructed when the effective gravitational coupling is varied. While the first branch exists for $\kappa \in [0; 1.268]$, the successive branches exist on smaller and smaller intervals of κ , e.g. the second branch for $\kappa \in [0.312; 1.268]$, the third for $\kappa \in [0.312; 0.419]$ and the fourth for $\kappa \in [0.395; 0.419]$. Further branches can be constructed in the interval $\kappa \in [0.395; 0.419]$, but have not been determined in detail. The endpoint of the branches is reached when the interval in κ shrinks to a point at $\kappa = \kappa_{cr}$. It has been noticed in [9] that the gauge field function $H_2(r) = H_4(r) = K(r)$ becomes oscillating around a fixed point. The number of oscillations increases along successive branches and becomes infinite in the limit $\kappa \rightarrow \kappa_{cr}$.

For one fixed value of κ , we thus have one, two, three and four globally regular vortex solutions for $\kappa \in [0.312; 0.395]$, $\kappa \in [0.312; 0.395]$ and $\kappa \in [0.395; 0.419]$, respectively. The mass of the fundamental solution on the first (the "main") branch is lower than the mass of the solution on any successive branch for a fixed value of κ . We would thus expect the "higher" solutions to be unstable with respect to the fundamental solution.

3.1.2 Axially symmetric solutions

The spherically symmetric configurations admit axially symmetric generalisations, obtained by taking $n > 1$ in the latter ansatz. A general discussion of these solutions has been presented in [11]. Here we report new results for $n = 2$. While in [11] only one branch of solutions in x has been constructed, we have reconsidered this problem and managed to construct a second branch of deformed non-abelian vortices. While the first ("main") branch exists for $x \in [0 : 1.28]$, we constructed a second branch for $x \in [0.88 : 0.128]$. This is demonstrated in Figure 1, where we plot the mass of the solution per winding number $= 2$ as function of x . Clearly, the solutions on the second branch have higher energy than those on the main branch for the same value of x . We also show the values of the metric functions f and ω at the origin (with $\omega = 0$), $f(0)$ and $\omega(0)$. Clearly, the solutions on the two branches are different for one fixed value of x . $f(0)$ on the second branch of solutions is very close to zero. This is also demonstrated in Figure 2, where we compare the profiles of the metric functions f and ω for $x = 0.8$ on the two branches.

We believe that several more branches exist, but were unable to construct them. Again, the pattern of globally regular deformed vortex solutions is important to understand the domain of existence of the deformed black strings, which we will discuss below.

3.2 $m = 0$ black string configurations

3.2.1 Spherically symmetric solutions

Here we present a detailed analysis of the model studied in [10, 12]. In [10], black string solutions for a fixed value of the horizon value and varying gravitational coupling have been constructed. It has been found that the pattern of solutions is very similar to that observed for non-abelian vortices. Several branches of solutions exist and the extent of the branches in x gets smaller and smaller for successive branches. In [12], the gravitational coupling has been fixed to $\kappa = 0.5$ and the horizon radius has been varied. Two branches of solutions in x , which both exist for $x \in [0 : x_{\text{max}}]$ have been found with $x_{\text{max}} = 0.633$. In the limit $x \rightarrow 0$, the solutions on the first and second branch, respectively, correspond to the globally regular non-abelian vortex solution on the main and second branch of vortex solutions for fixed κ . It has been suggested in [12] that two branches in x exist for all fixed values of κ . The numerical results presented here confirm this expectation. In Figure 3 we show the domain of existence of the black string solutions in the $(-\kappa)$ -plane.

As is clearly seen from this figure, the critical behaviour of the solutions depends crucially on the choice of κ . For $\kappa \in [0 : 0.312]$ the solutions on the second branch tend to the Einstein-Maxwell-dilaton (EMD) solutions for a finite value of $x = x_{\text{cr}}$. This is demonstrated in Figure 4 for $\kappa = 0.2$, where the value of the gauge field function $H_2(x) = H_4(x) - K(x)$ at the horizon, $K(x_{\text{cr}})$, is shown as function of x . Clearly, the second branch of solutions ends at $K(x_{\text{cr}}) = 0$, which together with the boundary conditions at infinity tells us that $K(x) = 0$.

In addition, the value of the gauge field function ω_1 at x_{cr} tends to one for $x \rightarrow x_{\text{cr}}$ (see Figure 5) such that $\omega_1(x) = 1$. The gauge field is thus trivial and becomes that of an EMD solution. At the same time, the metric function f , which in the 4-dimensional picture corresponds to a dilaton, tends to the dilaton field of the corresponding EMD solution. This can e.g. be seen by comparison of the value of $f(x_{\text{cr}})$ (see Figure 6) with that of the EMD solution with same horizon value.

For $\kappa = 0.5$, the picture is completely different. Again, two branches of solutions exist, but now the second branch extends all the way back to $x = 0$. $K(x)$ and $\omega_1(x)$ tend back to one, respectively zero, the values of the globally regular vortex solution (see Figure 4 and Figure 5). The solutions reach the globally regular vortex solutions discussed in Section 3.2 for $x \rightarrow 0$. However, Figure 5 shows that the terminating solution of the second branch is different from that of the first branch. The limiting solutions of the first, respectively second branch correspond to the fundamental and second globally regular vortex solution. The reason why the second branch terminates in the second regular solution relates to the fact that only two different globally regular vortex solutions exist for $\kappa = 0.5$. If we had chosen a value of κ for which more than two vortex solutions exist, the second branch of black strings would terminate into the "highest" available solution, e.g. for $\kappa \in [0.395 : 0.419]$, the second branch would terminate in the 4th globally regular solution. This behaviour

Table 1: Maximal and critical value of x for deformed black string solutions ($n = 2$)

	x_{max}	x_{cr}	Bifurcation of second branch with
0.1	1.35	0.88	EM D
0.3	1.33	0.72	EM D
0.5	1.30	0.0	regular
1.0	0.845	0.0	regular

is demonstrated in Figure 3, where we indicate with "\2.", "\3." "\4." at which globally regular vortex solution the second branch of black strings terminates.

3.2.2 Axially symmetric solutions

We have constructed deformed black string solutions for $n = 2$ for three fixed values of α . Our results are shown in Figures 6-10, where we give the values of the gauge field functions H_2 , ϕ_1 and of the metric functions ρ and J at the horizon as functions of the area parameter x . First, we remark that -apart from the metric function J -the curves can hardly be distinguished for different values of α . Very similar to what has been observed in the case $n = 1$, two branches of solutions exist. Again, the limiting behaviour depends strongly on the choice of α . Since we don't have a detailed analysis of the branch structure of the $n = 2$ globally regular vortex-type configuration, we cannot make a precise prediction to which solution the second branch tends. However, we can make qualitative statements about the domain of existence of the deformed black strings in the $(-x)$ -plane. We find that for $\alpha = 0.1$, the second branch terminates into an EM D solution with $H_2(x)$ tending to zero at a finite $x = x_{\text{cr}}$ (see Figure 7), $\phi_1(x)$ reaching one in this limit (see Figure 8), while ρ and J take their respective values of the corresponding EM D solution (see Figure 9 and Figure 10). Note that the EM D is a spherically symmetric solution, the curves for different α should thus meet at x_{cr} . This is what we noticed in our computation. For $\alpha = 0.5$ and $\alpha = 1.0$, the situation is different. We find that the second branch of black string solutions reaches back to $x = 0$, where it tends to a globally regular vortex-type solution. Since we don't know the detailed branch structure of the globally regular $n = 2$ solution, we don't know which "higher" solution the limiting solution is. Clearly, the limiting solution is axially symmetric, which can be seen in Figure 10, where the curves for $j(x)$ (note that j is the transformed function given in Appendix B) ends at finite values for $x = 0$. If the solutions would be spherically symmetric the off-diagonal component of the metric tensor would be vanishing, i.e. $j = J = 0$, which clearly is not the case here.

The domain of existence of the deformed black strings is qualitatively very similar to that of the uniform black strings. The values for $n = 2$ are given in Table 1.

We give them axial horizon value x_{max} at which the two branches meet as well as the critical horizon value x_{cr} where the second branch of solutions ends. The last column indicates at which solution the second branch terminates. Clearly for $\alpha = 0.1$ and $\alpha = 0.3$, the second branch tends to the EM D solution for $x \rightarrow x_{\text{cr}}$, while for $\alpha = 0.5$ and $\alpha = 1.0$, the second branch extends all the way back to $x = 0$, where it bifurcates with the globally regular solution. We note when comparing the results for the deformed black strings with those for the uniform black strings that the former exist for much larger values of the horizon value.

In Figure 11, we show the ratio of the horizon circumference along the equator L_e and along the poles L_p , $\rho = L_e/L_p$ as function of x for three different values of α . This ratio is a direct measure for the deformation of the horizon of the black string solution. For $\alpha = 0.1$, ρ stays very close to one which, of course, is related to the weak gravitational coupling. For both $\alpha = 0.5$ and $\alpha = 1.0$, the deformation of the horizon is much stronger on the second branch as compared to the first branch. Interestingly, the maximal deformation of the $\alpha = 0.5$ solution is larger than that of the $\alpha = 1.0$ solution. This is likely related to the fact that the $\alpha = 0.5$ black string solutions have larger possible horizon values than the $\alpha = 1.0$ solutions.

In Figure 12, we show the temperature T and the entropy S of the deformed black strings ($n = 2$) as

functions of x . We present the figure only for $\alpha = 0.5$ because the curves differ hardly for different α (e.g. $\alpha = 0.2, \alpha = 1.0$). The numerics further indicates that, for fixed x , the solution with the lower mass possesses the lower temperature. The temperature tends to infinity in the limit $x \rightarrow 0$, while the entropy tends to zero. This is not surprising since as $x \rightarrow 0$ the event horizon area tends also to zero, while the temperature of a globally regular solution is arbitrary.

The dependence of the mass of the solutions of the parameter x is exhibited in Figure 13 for two values of α . In Figure 14 we present a plot of the tension of the solutions as a function of x for two values of α . One can see that the behaviour of σ resembles that of m , the tension on the upper branch being higher than the corresponding value on the lower branch. In Figure 15 the $(\alpha; n_t)$ phase diagram is presented for $\alpha = 0.1; \alpha = 0.5$. This type of phase diagram was proven important in classifying the non-uniform black strings and black holes on a cylinder [21]. One finds that these deformed black string solutions cover compact regions of the $(\alpha; n_t)$ plane. In particular there are solutions with $n_t > 1=2$, where $1=2$ is the vacuum value.

The energy density of the matter fields is angle dependent, and in particular is not constant at the horizon. The maximum of the energy density resides on the z axis, as seen in Figure 16, where a three-dimensional plot of the T_t^t component of the energy-momentum tensor is presented.

3.3 $m = 1$ black string configurations

A very different picture is found by taking $m = 1$ in the asymptotic boundary conditions, i.e.: $\alpha_1 = \cos \theta$, $\alpha_2 = \sin \theta$, the asymptotics of H_1 being fixed by (22) (here we consider the case $n = 1$ only, although a number of $n = 2$ configurations have been also studied with similar qualitative results). Different from $m = 0$, no spherically symmetric solutions are found for this set of boundary conditions.

Let us briefly recall the features of the corresponding vortex-type solutions discussed in [11]. The boundary conditions at infinity and at $r = 0; r = 2$ satisfied by these regular solutions are similar to the black hole case. The conditions (45) at $r = 0$ are also fulfilled except for the A_5 potentials, which satisfy $\cos \theta_{r=1} \sin \theta_{r=2} = 0; \sin \theta_{r=1} + \cos \theta_{r=2} = 0$.

In the limit $d \rightarrow 0$, a branch of $m = 1$ vortex-type solutions emerges from the uplifted version of the $d = 4$ static spacetime MA configurations in YMH theory [27]. This branch ends at a critical value $\alpha_{cr} = 0.65$. Apart from this fundamental branch, the $m = 1$ solutions admit also excited configurations, emerging in the $d \rightarrow 0$ limit (after a rescaling) from the spherically symmetric solutions with $A_5 = 0$ (corresponding after dimensional reduction to solutions of a $d = 4$ EYM-dilaton theory). The lowest excited branch (the only case discussed in [11]), originating from the one-node spherically symmetric solution, evolves smoothly from $\alpha = 0$ to α_{cr} where it bifurcates with the fundamental branch. The energy density $\rho = T_t^t$ possesses maxima at $z = d=2$ and a saddle point at the origin, and presents the typical form exhibited in the literature on MA solutions [28, 27]. The modulus of the fifth component of the gauge potential possesses always two zeros at $d=2$ on the z symmetry axis. The excited solutions become infinitely heavy as $d \rightarrow 0$ while the distance d tends to zero.

These regular solutions present black hole counterparts, which in a four dimensional perspective, share many properties with the corresponding EYM H black hole configurations with magnetic dipole hair [29]. For any fixed value of α , $0 < \alpha < \alpha_{cr}^{reg}$, we obtain two branches of black string solutions. Imposing a regular event horizon at a small radius x , the lower branch of black string solutions emerges from the corresponding lower branch globally regular EYM vortex-type solution. This branch of solutions extends to a maximal value $x_{max}(\alpha)$. Along this lower branch, the mass increases with increasing x (see Figure 23). Decreasing x from $x_{max}(\alpha)$, a second branch of solutions appears. Along this upper branch the mass decreases with decreasing x , reaching the regular upper branch MA solution, when $x \rightarrow 0$. We note that for the same event horizon radius, the mass of the upper branch solution is higher. In Figures 17-20 we illustrate the value of the functions H_2, H_1 , and J at x for two values of α . Similar to the $m = 0$ case, these plots do not exhibit a strong dependence on the value of α (except for $J(x)$). The metric function $J(r; \alpha)$ presents a nontrivial angular dependence, behaving asymptotically as $J = J_0 \sin^2 \theta = r$. Other branches of solutions may exist as well, in particular those emerging from multinode regular configurations.

In Figure 21, we show the ratio of the horizon circumference along the equator L_e and along the poles L_p , $\beta = L_e/L_p$ as function of x for $\alpha = 0.2$ and $\alpha = 0.5$. As seen in Figure 22, the Hawking temperature increases with decreasing r_h , diverging as $r_h \rightarrow 0$. While the entropy of the regular solutions is zero, it approaches a

maximal value at $r_{h(\max)}$ (). Figure 24 presents a plot of the tension of the solutions as a function of x for two values of α . As in the case of $m = 0$ solutions, the behaviour of T_t resembles that of T and the tension on the upper branch is higher than the corresponding value on the lower branch. In Figure 25 the $(\alpha; n_t)$ phase diagram is presented for $\alpha = 0.2$; $\alpha = 0.5$. We note again the existence of solutions with $n_t > 1=2$.

In Figure 26 we exhibit the energy density of a typical lower branch $m = 1$; $n = 1$ solution, with $\alpha = 0.2$, $r_h = 0.04$. Note the different shape of T_t as compared to the $m = 0$ case, with two extrema on the z axis.

3.4 $A_5 = 0$ solutions

It is interesting to consider the following consistent reduction of the ansatz (11)

$$A_1 = A_2 = 0; \quad (48)$$

(i.e. no Higgs field will appear in the $d = 4$ theory), in which case one should also set $W = 0$.

The four dimensional picture one finds from (7) corresponds to a EYM-dilaton system

$$I_4 = \int d^4x \sqrt{-g} \left[\frac{1}{4G} R - \frac{1}{2} \partial_\mu r \partial^\mu r - \frac{1}{2g^2} \text{Tr} F_{\mu\nu} F^{\mu\nu} \right]; \quad (49)$$

with a particular coupling between dilaton and gauge field.

Both particle like and black hole solutions of this system are known to exist. Here we'll review their basic properties from a five dimensional perspective. Although the configurations are again indexed by the set of two integers $(m; n)$, the $A_5 = 0$ EYM solutions present a number of distinct features. First, it appears that there are no $m = 0$ finite mass nonabelian vortices or black string solutions. This can easily be proven for configurations which are spherically symmetric in four dimensions by applying the arguments in [30]. This implies that, without a Higgs field, there are no nonabelian monopole solutions in the EYM D system (49).

However, nontrivial solutions are found by taking the $m = 1$ set of boundary conditions for the matter fields H_i . First, for $n = 1$, the four dimensional solutions are again spherically symmetric being discussed in [31]. The corresponding $d = 5$ vortices and black strings are parametrized by the number k of nodes of the gauge function $K(r)$, the extremal abelian solution being approached as k tends to infinity. All these solutions turn out to be unstable in linearized perturbation theory [31].

As found in [32], [33], these configurations admit axially symmetric generalisations, obtained for a winding number $n > 1$. Different from the $A_5 \neq 0$ case, here we find black string solutions for any radius r_h of the horizon. These deformed solutions are characterized by two integers, the winding number n and the node number k of the purely magnetic gauge field. The mass of these solutions increases with $n; k$. With increasing node number the magnetically neutral black string solutions form sequences tending to limiting solutions with magnetic charge n , corresponding in a $d = 4$ picture to EMD black hole solutions. Although no proof exists in the literature, we expect these configurations to be unstable, too.

A general $(2m; n)$ set of $d = 4$ EYM solutions have been discovered recently in [34], [35]. There the gauge potentials H_i satisfy a complicated m -dependent set of boundary conditions. These solutions presumably admit a dilatonic generalization within the theory (49), describing in a $d = 5$ picture new sets of nonabelian vortices and black strings.

4 New $d = 4$ solutions from boosted $d = 5$ configurations

For vacuum solutions extremizing (7), it has been known for some time that, by taking the product of the $d = 4$ Schwarzschild solution with a circle and boosting it in the fifth direction, the entire family of electrically charged (magnetically neutral) KK black holes is generated.

As remarked in [11], a similar construction can be applied to the solutions of the $d = 4$ EYM H-U (1)-dilaton theory (7). Starting with a purely magnetic $d = 4$ static configuration $(\alpha; A; W; \dots)$, and uplifting it according to (5), (6), one finds in this way a vortex-type (or black string) solution of the $d = 5$ EYM theory. The next step is to boost this solution in the $(z; t)$ plane

$$z = \cosh \chi Z + \sinh \chi t; \quad t = \sinh \chi Z + \cosh \chi t; \quad (50)$$

The dimensional reduction of this EYM configuration along the Z direction provides a new solution in the $d = 4$ EYM H-U (1)-dilaton theory. For the specific ansatz considered in this paper one finds

$$\begin{aligned} d^2 &= dx dx = e^{a(\cdot)} dt (d^2 \sinh^2 W, d')^2 + e^{a(\cdot)} d^2 \\ &= f (d^2 \sinh^2 W, d')^2 + \frac{q}{f} (dr^2 + r^2 d^2) + \frac{1}{f} r^2 \sin^2 \theta d^2; \end{aligned} \quad (51)$$

the new functions being expressed in terms of the initial solution as

$$f = \frac{1}{q} \log(\cosh^2 e^{3a} f \sinh^2); \quad (52)$$

$$f = f \cosh^2 e^{3a} f \sinh^2; \quad q = q; \quad l = l; \quad (53)$$

for the dilaton and metric functions, while the expression of the new gauge potentials is

$$\begin{aligned} A_r &= A_r; \quad A_\theta = A_\theta; \quad A_\phi = A_\phi - 2W, \quad \frac{e^{2a} f \sinh^2}{e^{2a} \cosh^2 e^{a} f \sinh^2}; \\ A &= \sinh \frac{e^{a} f}{e^{2a} \cosh^2 e^{a} f \sinh^2}; \\ W, &= \frac{e^{2a} \cosh W}{e^{2a} \cosh^2 e^{a} f \sinh^2}; \quad W = \frac{1}{2} \frac{(e^{2a} e^{a} f) \sinh \cosh}{e^{2a} \cosh^2 e^{a} f \sinh^2}; \end{aligned} \quad (54)$$

The new Higgs is

$$= \cosh; \quad (55)$$

To support a boosting given by a parameter β , one finds the condition

$$e^{3a} f \tanh^2 < 1 \quad (56)$$

which turns out to be satisfied by all considered configurations.

For axially symmetric solutions, the new four dimensional line element presents a nonzero extradiagonal metric component $dt dr$, and thus describes a rotating spacetime. Also, the electric potentials A_θ of the $d = 4$ SU(2) field is nonzero, being proportional to the Higgs field.

This procedure applied to globally regular MM and MA configurations generates charged rotating solutions. As discussed in [11], although they will rotate locally, the total angular momentum of the MM solutions is zero, and the spacetime consists in two regions rotating in opposite directions. The solutions with a zero net magnetic charge possess a nonvanishing angular momentum proportional to the magnetic charge (the rotating solutions found recently in EYM H theory present the same qualitative picture [36]). In this construction, the causal structure is not affected by the boosting procedure, i.e.: $\beta > 0$, (no closed timelike curves) and no event horizon occurs in the new solutions (here we take also $-1 < \beta < 1$ and ignore the causal problems implied by performing the transformation (50) with an extra- S^1 direction).

The same procedure applied to static, axially symmetric black hole configurations gives rotating black hole solutions. For the new line element (51), the event horizon is a Killing horizon of the Killing vector $\partial_t = \partial_t + \Omega_H \partial_\phi$, [37]. Here $\Omega_H = \beta$, $\beta = \beta$, (evaluated at the event horizon) corresponds to the event horizon velocity. The resulting solutions have a number of interesting properties. For the specific ansatz used in (51), one can see that the event horizon location is unaffected by the boosting procedure $(r_h) = 0$, while $\Omega_H = 0$, i.e.: the event horizon is not rotating with respect to infinity. Therefore the causal structure of the initial solution is unchanged by the generation procedure, and no ergoregion is found, since $f > 0$ outside the event horizon. Moreover, similar to the regular case, the ADM angular momentum of the black hole solutions with a nonvanishing magnetic charge is zero, although they rotate locally, while the $m = 1$ solutions have a nonzero angular momentum.

A detailed discussion of the properties of the $d = 4$ EYM H-U (1)-dilaton rotating solutions generated by boosting static axially symmetric configurations in the x^5 -direction will be given elsewhere.

4.1 d = 4 spherically symmetric dyonic black holes

For the rest of this Section we'll concentrate on the simpler spherically symmetric case. The black string solutions of this model are discussed in [10]. The four dimensional initial picture is straightforward, and consists in magnetic monopole black holes in EYM H-dilaton theory (i.e: no U(1) eld $W = 0$). After boosting, the new d = 4 solutions correspond to black hole dyons, which, different from other cases discussed in the literature have also a nonvanishing U(1) electric potential (the spherically symmetric, globally regular counterparts of these solutions have been constructed in [38] by directly solving the eld equations).

For the particular case of spherical symmetry, the relations (51) read

$$d^2 = -f(r)dr^2 + \frac{q(r)}{f(r)} dr^2 + r^2 d^2 + r^2 \sin^2 \theta d\theta^2; \quad (57)$$

the new metric functions being determined by (52). The four dimensional YM elds are

$$A_r = 0; A_\theta = (1 - K(r))^{-1/2}; A_\phi = (1 - K(r))^{-1/2} \sin \theta; A_t = \sinh^{-1}(r) e^{\frac{1}{r}}; \quad (58)$$

$K(r)$ being the magnetic nonabelian potential of the initial monopole solution. The transformed Higgs eld of the four dimensional theory is $H = \cosh^{-1}$, while the new dilaton is given by

$$e^a = e^{a(r)} \frac{q}{\cosh^2} e^{-3a(r)f \sinh^2}; \quad (59)$$

One can see that, similar to the solutions of the (E-)YM H theory, the magnitude at infinity of the electric potential is restricted to be less than that of the Higgs eld. The Maxwell eld which appears as a result of the boosting procedure possesses a nonvanishing electric potential W which can be read from (54).

The location of the event horizon is unaffected by boosting, while the relation between the Hawking temperature and entropy of the dyonic black holes and the corresponding quantities of the monopole solutions is $T = T_0 \cosh^{-1}$, $S = S_0 \cosh^{-1}$. The properties of a dyon solution can be predicted from the "seed" configuration, in particular the domain of existence in the $(r; r_h)$ plane. The magnetic potential $K(r)$ vanishes at infinity which gives a unit magnetic charge, while the nonabelian electric charge determined as $Q_e^{(n)} = \lim_{r \rightarrow \infty} \int_{S^2} r^2 \partial_r A$ is

$$Q_e^{(n)} = \frac{\sinh}{2} (3ad - (2h_1 + M) + (3ad - 2M) \cosh 2); \quad (60)$$

(where $h_1 = \lim_{r \rightarrow \infty} r^2 \partial_r$). The ADM mass and the abelian charge of these solutions are determined in terms of the mass M and dilaton charge d of the initial configurations

$$M = M_0 (\cosh^2 - \frac{1}{2} \sinh^2) - \frac{3}{4} ad \sinh^2; Q_e^{(a)} = \frac{1}{4} (3ad - 2M) \sinh 2; \quad (61)$$

while the new dilaton charge (defined as $d = \lim_{r \rightarrow \infty} \int_{S^2} r^2 \partial_r$) is

$$d = d_0 (\cosh^2 + \frac{1}{2} \sinh^2) - \frac{1}{a} M \sinh^2; \quad (62)$$

Other properties of these solutions can easily be deduced from the analysis presented in Section 3.2.1.

5 Conclusions

In this paper we have considered black string solutions in the d = 5 SU(2) EYM theory. From a four dimensional perspective, these solutions correspond to spherically and axially symmetric black holes sitting inside the center of (multi)monopoles and monopole-antimonopole pairs.

For a class of regular configurations corresponding to solutions with a net magnetic charge in the d = 4 theory, we have presented new results for a second branch of solutions. The domain of existence in the $(r; x)$ -plane of the black string counterparts of these configurations has been determined. We find that when the

gravitational coupling is fixed, two branches of solutions exist. The second branch terminates into Einstein-Maxwell-dilaton solutions for values of the gravitational coupling for which only one globally regular vortex solution exists, respectively into the "highest" available globally regular vortex solution for values of γ where more than one vortex solution exists. We have also presented numerical arguments for the existence of a different type of $d = 5$ EYM black strings, corresponding in a four dimensional picture to black holes located in between a monopole-antimonopole pair.

In this context, we have proposed a simple procedure to generate new $d = 4$ electrically charged solutions with nonabelian matter fields starting with static $d = 5$ EYM black string solutions.

In Appendix A an argument has been presented against the existence of hyperspherically symmetric black hole solution with reasonable asymptotics in $SU(2)$ Einstein-Yang-Mills theory in $d = 5$. Therefore, the solutions discussed in this paper as well the regular counterparts represent the simplest nontrivial configurations in $d = 5$ EYM theory, they providing also another counterexample to the no hair conjecture in five dimensions.

Concerning the stability of these nonabelian black holes, we expect the $m = 0$ solutions with a nonzero magnetic charge to be stable in a certain region of the parameter space. However, all $m = 1$ configurations are presumably unstable, like their MA -at space counterparts [27].

One may speculate about the existence of nonuniform vortices and black strings with nonabelian matter, with a dependence on the extra z -coordinate. Similar to the vacuum case, we expect these solutions to emerge from the uniform EYM configurations for a critical value of the mass. However, the five dimensional gravity presents also black ring solutions, with an horizon topology $S^2 \times S^1$, which approaches at infinity the flat M^5 background. A vacuum black ring can be constructed in a heuristic way by taking the neutral black string, bending the extra dimension and spinning it along the circle direction just enough so that the gravitational attraction is balanced by the centrifugal force. This is a neutral rotating ring, obtained in Ref. [39] as a solution of the $d = 5$ vacuum Einstein equations. Generalizations of this solution for an abelian matter content are known in the literature. Nonabelian versions of these configurations are also likely to exist, and will necessarily have an electric field. However, the construction of such solutions represents a difficult challenge.

Acknowledgements

YB is grateful to the Belgian FNRS for financial support. BH thanks the University of Mons, where part of this work was done, for hospitality. The work of ER is carried out in the framework of Enterprise-Ireland Basic Science Research Project SC/2003/390 of Enterprise-Ireland.

References

- [1] F. R. Tangherlini, *Nuovo Cimento* 27 (1963), 636.
- [2] G. T. Horowitz and A. Strominger, *Nucl. Phys. B* 360 (1991), 197.
- [3] R. Gregory and R. Laamamme, *Phys. Rev. Lett.* 70 (1993) 2837 [[arXiv:hep-th/9301052](#)].
- [4] G. T. Horowitz and K. Maeda, *Phys. Rev. Lett.* 87 (2001) 131301 [[arXiv:hep-th/0105111](#)].
- [5] S. S. Gubser, *Class. Quant. Grav.* 19 (2002) 4825 [[arXiv:hep-th/0110193](#)].
- [6] T. Wiseman, *Class. Quant. Grav.* 20 (2003) 1137 [[arXiv:hep-th/0209051](#)].
- [7] T. Harmark and N. A. Obers, [arXiv:hep-th/0503020](#).
- [8] M. S. Volkov and D. V. Gal'tsov, *Phys. Rept.* 319 (1999) 1 [[arXiv:hep-th/9810070](#)].
- [9] M. S. Volkov, *Phys. Lett. B* 524 (2002) 369 [[arXiv:hep-th/0103038](#)].
- [10] B. Hartmann, *Phys. Lett. B* 602 (2004) 231 [[arXiv:hep-th/0409006](#)].

- [1] Y. Brihaye, B. Hartmann and E. Radu, Phys. Rev. D 71 (2005) 085002 [arXiv:hep-th/0502131].
- [2] Y. Brihaye and B. Hartmann, arXiv:gr-qc/0503102.
- [3] G. T. Horowitz, arXiv:hep-th/0205069.
- [4] Y. Brihaye, A. Chakrabarti, B. Hartmann and D. H. Tchrakian, Phys. Lett. B 561 (2003) 161 [arXiv:hep-th/0212288].
- [5] N. Ouyama and K. I. Maeda, Phys. Rev. D 67 (2003) 104012 [arXiv:gr-qc/0212022].
- [6] P. Forgacs and N. S. Manton, Commun. Math. Phys. 72 (1980) 15,
P. G. Bergmann and E. J. Flaherty, J. Math. Phys. 19 (1978) 212.
- [7] D. Garofalo, G. T. Horowitz and A. Strominger, Phys. Rev. D 43 (1991) 3140 [Erratum: ibid. D 45 (1992) 3888].
- [8] J. X. Lu, Phys. Lett. B 313 (1993) 29 [arXiv:hep-th/9304159].
- [9] R. C. Myers, Phys. Rev. D 60 (1999) 046002 [arXiv:hep-th/9903203].
- [20] S. W. Hawking and G. T. Horowitz, Class. Quant. Grav. 13 (1996) 1487 [arXiv:gr-qc/9501014].
- [21] T. Harmark and N. A. Obers, Class. Quant. Grav. 21 (2004) 1709 [arXiv:hep-th/0309116].
- [22] G. W. Gibbons and S. W. Hawking, Phys. Rev. D 15 (1977) 2752.
- [23] R. B. Mann, Found. Phys. 33 (2003) 65 [arXiv:gr-qc/0211047].
- [24] M. Visser, Phys. Rev. D 48 (1993) 583 [arXiv:hep-th/9303029].
- [25] U. Ascher, J. Christiansen, R. D. Russell, Math. of Comp. 33 (1979) 659;
U. Ascher, J. Christiansen, R. D. Russell, ACM Trans. 7 (1981) 209.
- [26] W. Schonauer and R. Wei, J. Comput. Appl. Math. 27, 279 (1989);
M. Schauder, R. Wei and W. Schonauer, The CAD SOL Program Package, Universitat Karlsruhe, Interner Bericht Nr. 46/92 (1992);
W. Schonauer and E. Schnepf, ACM Trans. on Math. Soft. 13, 333 (1987).
- [27] B. Kleihaus and J. Kunz, Phys. Rev. D 61 (2000) 025003 [arXiv:hep-th/9909037].
- [28] B. Kleihaus and J. Kunz, Phys. Rev. Lett. 85 (2000) 2430 [arXiv:hep-th/0006148].
- [29] B. Kleihaus and J. Kunz, Phys. Lett. B 494 (2000) 130 [arXiv:hep-th/0008034].
- [30] P. Bizon, O. T. Popp, Class. Quant. Grav. 9 (1992) 193;
A. A. Ershov, D. V. Galtsov, Phys. Lett. A 150 (1990) 159.
- [31] G. V. Lavrelashvili and D. Maison, Nucl. Phys. B 410 (1993) 407.
- [32] B. Kleihaus and J. Kunz, Phys. Rev. D 57 (1998) 834 [arXiv:gr-qc/9707045].
- [33] B. Kleihaus and J. Kunz, Phys. Rev. D 57 (1998) 6138 [arXiv:gr-qc/9712086].
- [34] R. Ibádov, B. Kleihaus, J. Kunz and M. Wirsching, arXiv:gr-qc/0507110.
- [35] R. Ibádov, B. Kleihaus, J. Kunz and Y. Shnir, Phys. Lett. B 609 (2005) 150 [arXiv:gr-qc/0410091].
- [36] B. Kleihaus, J. Kunz and U. Neemann, arXiv:gr-qc/0507047.
- [37] R. M. Wald, General Relativity, Chicago, Chicago Univ. Press, (1984).
- [38] Y. Brihaye and E. Radu, Phys. Lett. B 605 (2005) 190 [arXiv:hep-th/0409065].
- [39] R. Emparan and H. S. Reall, Phys. Rev. Lett. 88 (2002) 101101 [arXiv:hep-th/0110260].

Appendix A : N o d = 5 spherically sym m etric black hole solutions

Follow ing the notations in [15], we consider a static, spherically sym m etric ve-dim ensional spacetime, with a metric given in Schwarzschild coordinates by

$$ds^2 = -f(r)e^{2\gamma(r)}dt^2 + \frac{dr^2}{f(r)} + r^2(d\theta^2 + \sin^2\theta d\phi^2 + \sin^2\theta d\psi^2); \quad (63)$$

where

$$f(r) = 1 - \frac{r_h^2}{r^2}; \quad (64)$$

For black hole solutions $f(r_h) = 0$ for some $r_h > 0$, while $f'(r_h) > 0$ and $\gamma(r_h)$ stays finite.

The construction of a spherically sym m etric Yang-M ills ansatz for a gauge group $SU(2)$ has been carefully discussed in [15]. The expression of the nonabelian connection in this case is

$$\begin{aligned} A_r^a &= 0; \quad A^\theta_a = (0; 0; w); \quad A^\phi_a = (w \sin\theta; \cos\theta; 0); \\ A_\psi^a &= (\cos\theta \sin\psi; w \sin\theta \sin\psi; \cos\theta); \quad A_t^a = 0; \end{aligned} \quad (65)$$

in terms of only one function $w(r)$. With the above ansatz, we find the Einstein-Yang-M ills equations

$$\begin{aligned} 0 &= 2r f w'' + \frac{(1 - w^2)^2}{r^2}; \quad 0 = \frac{2}{r} w''; \\ \frac{1}{r} (r f e^{-\gamma} w^0)' + \frac{2}{r^2} e^{-\gamma} w (1 - w^2) &= 0; \end{aligned} \quad (66)$$

Introducing a new variable

$$z = 2 \ln r \quad (67)$$

the equations (66) imply the relations

$$\frac{d}{dz} = 4f \frac{dw}{dz}^2 + 1 - w^2 \quad (68)$$

$$f \frac{d^2 w}{dz^2} + e^{-z} e^{-z} (1 - w^2)^2 \frac{dw}{dz} + \frac{1}{2} w (1 - w^2) = 0; \quad (69)$$

with $f = 1 - e^{-z}$; the function γ being eliminated. To find a proof for the nonexistence of finite mass solutions of the above system, following [15], it is convenient to introduce the function

$$E = \frac{1}{2} f \frac{dw}{dz}^2 - \frac{1}{8} (1 - w^2)^2; \quad (70)$$

satisfying the equation

$$\frac{dE}{dz} = 4e^{-z} \frac{dw}{dz}^2 - E + \frac{1}{8}; \quad (71)$$

It is obvious that $E(r_h) < 0$; at the same time, as proven in [15], $E \rightarrow +0$ as $r \rightarrow \infty$, for finite mass solutions. Therefore, if the solution is regular everywhere, E must vanish at some finite point z_0 , and $dE/dz = 0$ there (when there are several positive roots of E , we take the largest one). However, another point should exist $z_1 > z_0$ such that $dE/dz = 0$ i.e. the function E should present a positive maximum for some value of z . Now we integrate the equation (71) between z_0 and z_1 and find

$$E(z_1) = 4 \int_{z_0}^{z_1} e^{-z} \frac{dw}{dz}^2 - E + \frac{1}{8} dz < 0; \quad (72)$$

which contradicts $E(z_1) > 0$. Therefore $E(z)$ should vanish identically and one finds no $d = 5$ finite mass, spherically symmetric EYM configurations. Note that this argument does not exclude the existence of configurations with a diverging mass functions as $r \rightarrow 1$. In fact, such solutions can easily be found and share many properties with the configurations without an event horizon discussed in [9].

Appendix B : Relation to a previous EYM string ansatz

The $m = 0$ deformed black strings discussed in Ref. [12] have been found for a slightly different ansatz. While the ansatz (5), (6) admits a straightforward KK picture and is useful for the determination of the corresponding rotating solutions, the notation of [12] turned out to be more convenient for numerical computation of $m = 0$ configurations.

For completeness, we present here the relation between these two ansätze. The d -dimensional metric parametrization used in [12] is

$$ds^2 = e^{2\alpha} \left(f dt^2 + \frac{m}{f} (dr^2 + r^2 d\Omega^2) + \frac{l}{f} r^2 \sin^2 \theta (d\phi + j dz)^2 + e^2 dz^2 \right); \quad (73)$$

while the YM matter ansatz corresponds to

$$A dx^\mu = \frac{1}{2gr} \left(H_1 dr + (1 - H_2) r d\theta + H_3 r d\phi + (1 - H_4) r \sin \theta d\phi' \right) + \tilde{\alpha}_1 \frac{1}{r} + \tilde{\alpha}_2 \frac{1}{r} dz \quad (74)$$

where $f, l, m, j, H_i, i = 1; 2; 3; 4$ and $\tilde{\alpha}_1, \tilde{\alpha}_2$ are again functions of r and θ only. They are related to the "untilded" functions appearing in (5), (6) as follows:

$$\begin{aligned} e^{\alpha} &= e^{-\alpha} \left(1 + e^{-3} \frac{l}{f} j^2 r^2 \sin^2 \theta \right)^{1/2}; \quad J = \frac{j l}{2 f} e^{-3} r^2 \sin^2 \theta \left(1 + e^{-3} \frac{l}{f} j^2 r^2 \sin^2 \theta \right)^{1/2}; \\ f &= f \left(1 + e^{-3} \frac{l}{f} j^2 r^2 \sin^2 \theta \right)^{1/2}; \quad m = m \left(1 + e^{-3} \frac{l}{f} j^2 r^2 \sin^2 \theta \right)^{1/2}; \quad l = l \end{aligned} \quad (75)$$

for the metric functions and

$$H_1 = H_1; \quad H_2 = H_2; \quad H_3 = H_3 + \frac{2g J}{n \sin \theta}; \quad H_4 = H_4 - \frac{2g J}{n \sin \theta}; \quad \alpha_1 = \tilde{\alpha}_1; \quad \alpha_2 = \tilde{\alpha}_2 \quad (76)$$

for the gauge fields functions. Of course, the final results are the same for both ansätze.

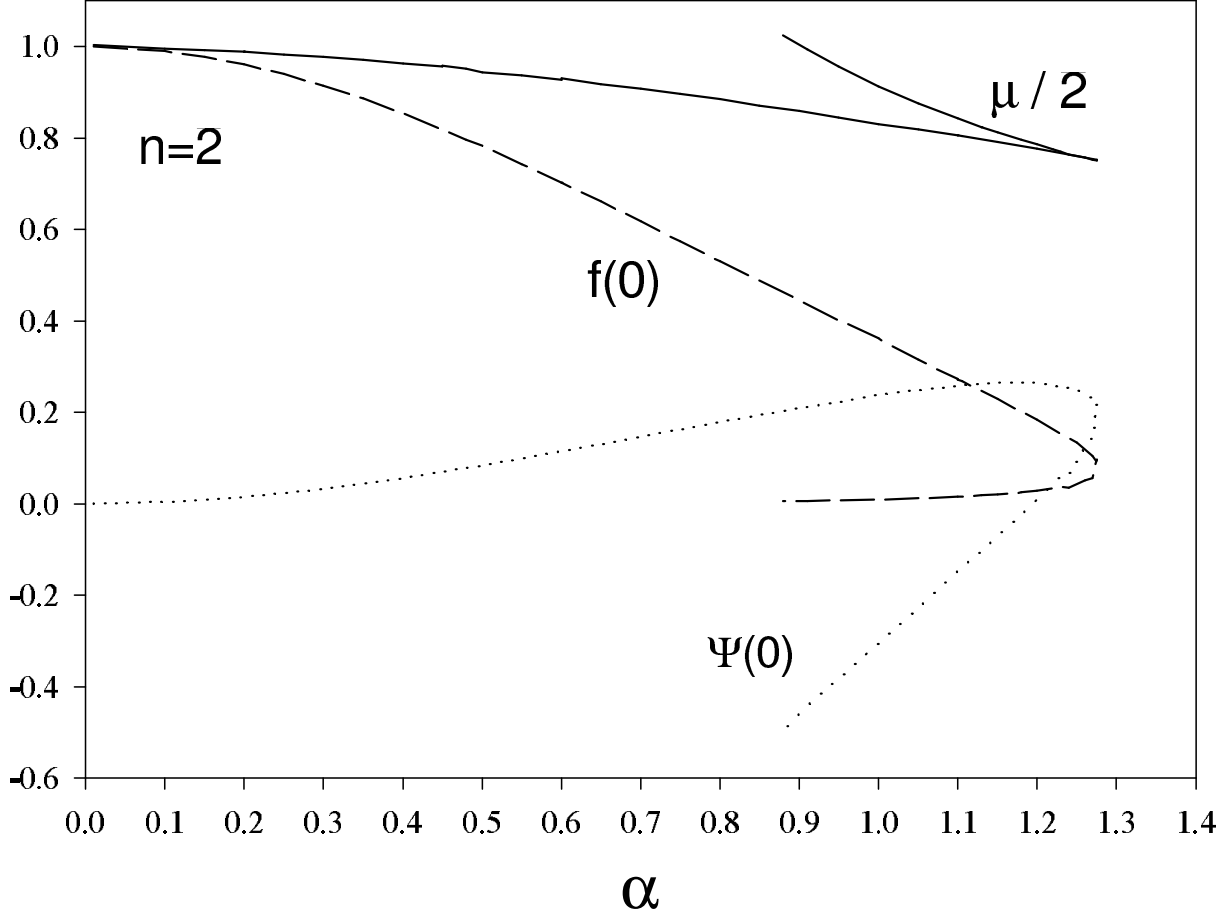


Figure 1. The value of the metric functions f , at the origin (with $\alpha = 0$), $f(0)$, $\Psi(0)$ are shown as function of α for the deformed non-abelian vortices with $m = 0$; $n = 2$. The upper and lower curve corresponds to the 1., respectively 2. branch of solutions. Also shown is the mass per winding number of the solutions, $\mu/2$, where the 1. branch has lower energy than the 2. branch.

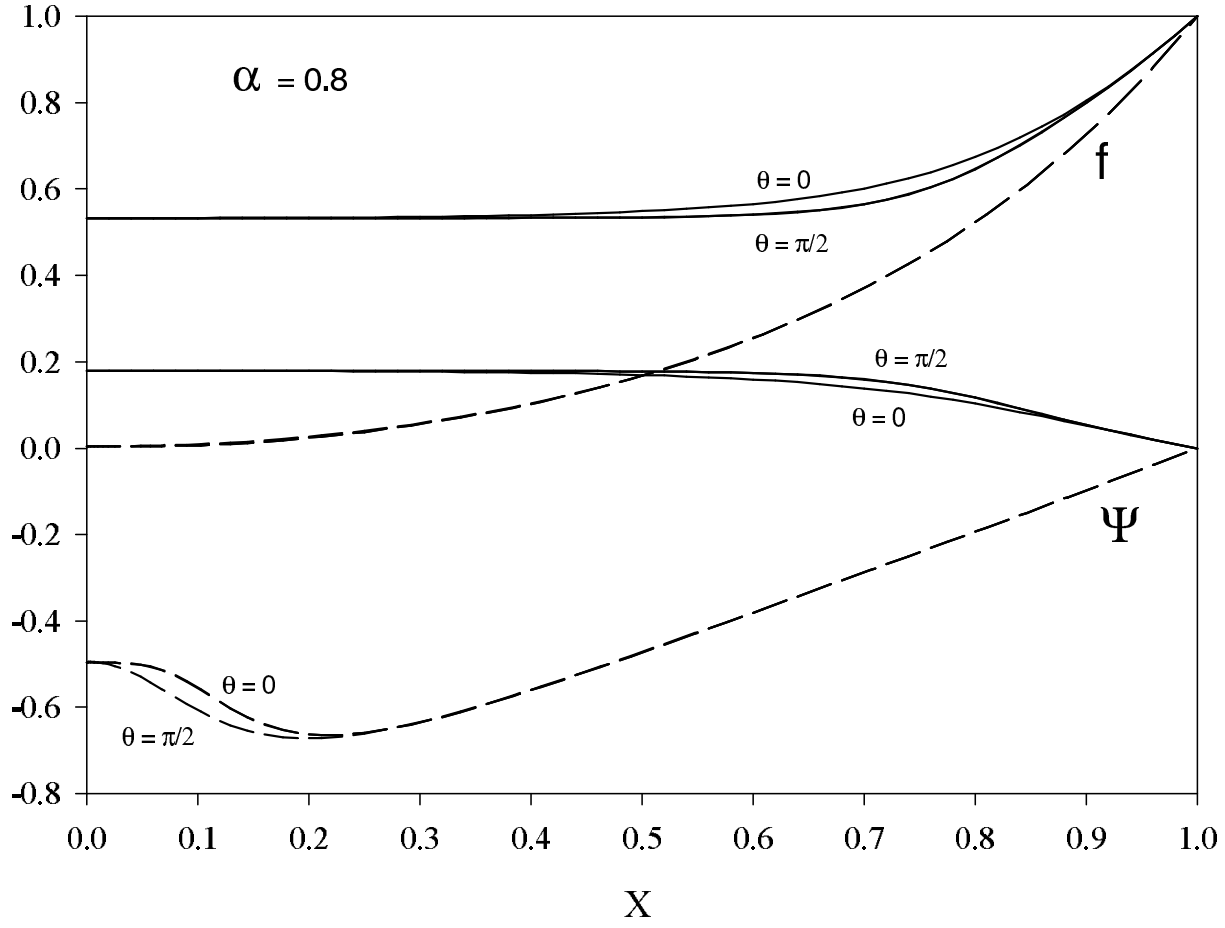


Figure 2. The profiles of the metric functions f and Ψ are shown for $\alpha = 0.8$ on the first ("main") branch (solid) and on the second branch (dashed) of $m = 0$ non-abelian deformed vortex solutions ($n = 2$). x here denotes the compactified coordinate $x = r/(1+r)$. Note that the two solid curves close to each other distinguish between $\theta = 0$ and $\theta = \pi/2$.

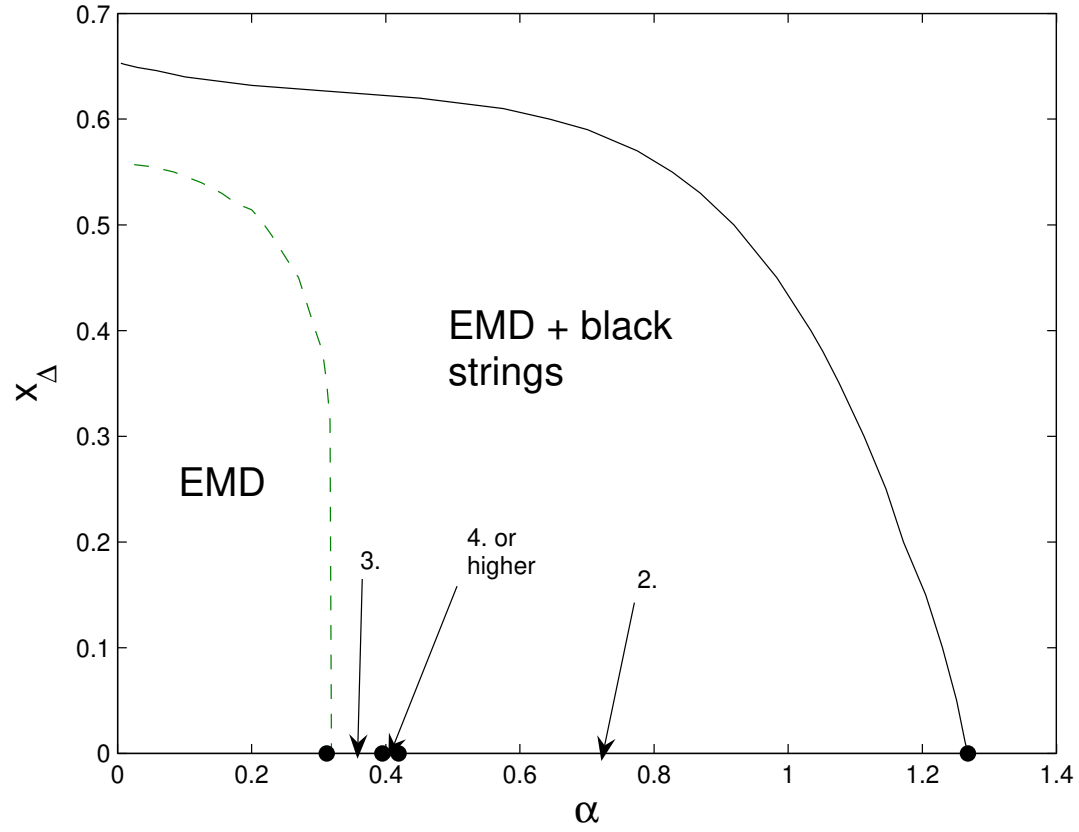


Figure 3. The domain of existence of the $m = 0$ uniform black string solutions in the (α, x_Δ) -plane is shown. "2.", "3." and "4. or higher" indicate to which non-abelian vortex solution the black strings on the second x_Δ -branch tend in the limit $x_\Delta \rightarrow 0$.

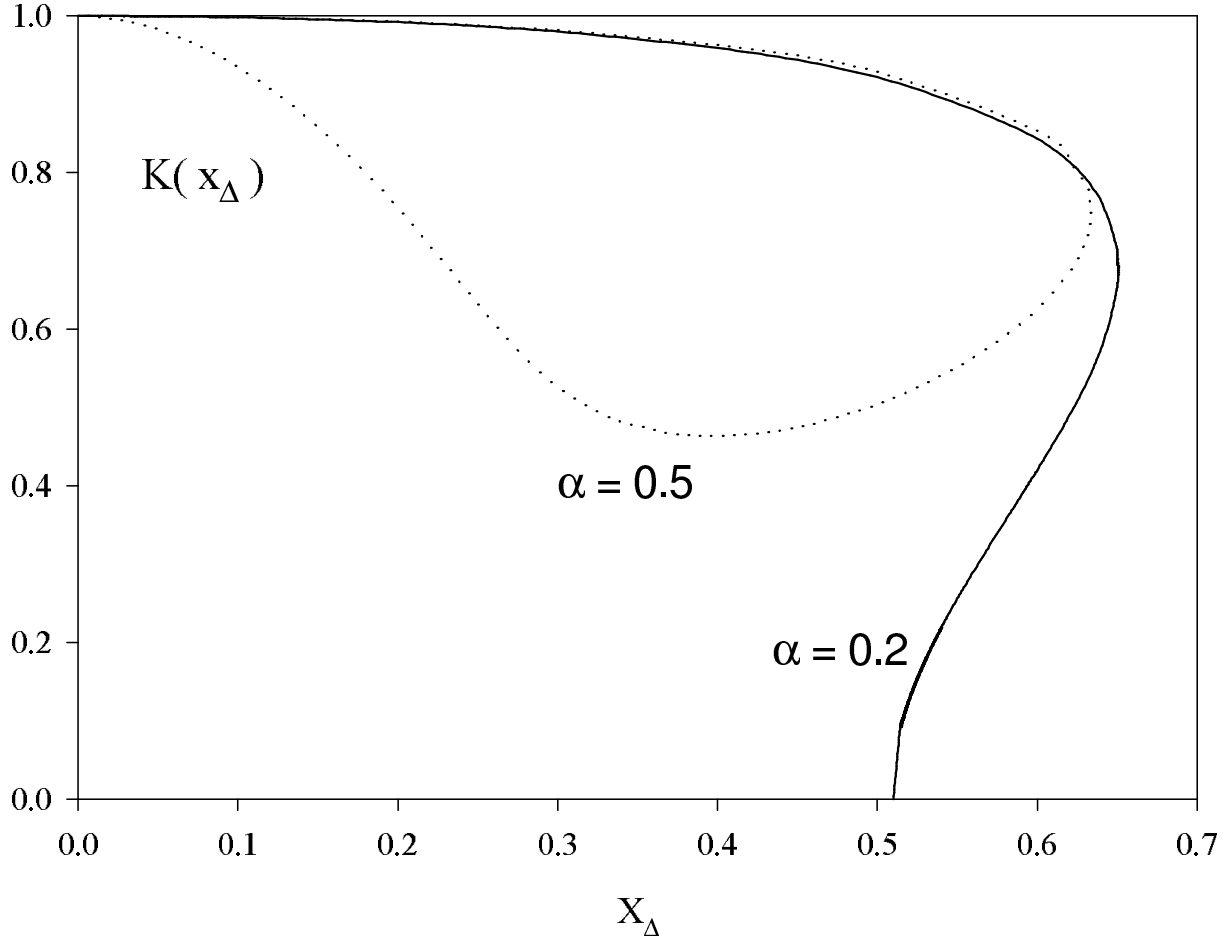


Figure 4. The value of the gauge field function of the uniform black string ($m = 0$; $n = 1$) at the horizon $H_2(x) = H_4(x)$ $K(x)$ is shown as function of x for $\alpha = 0.2$ and $\alpha = 0.5$. The upper and lower curves correspond to the 1., respectively 2. branch of solutions.

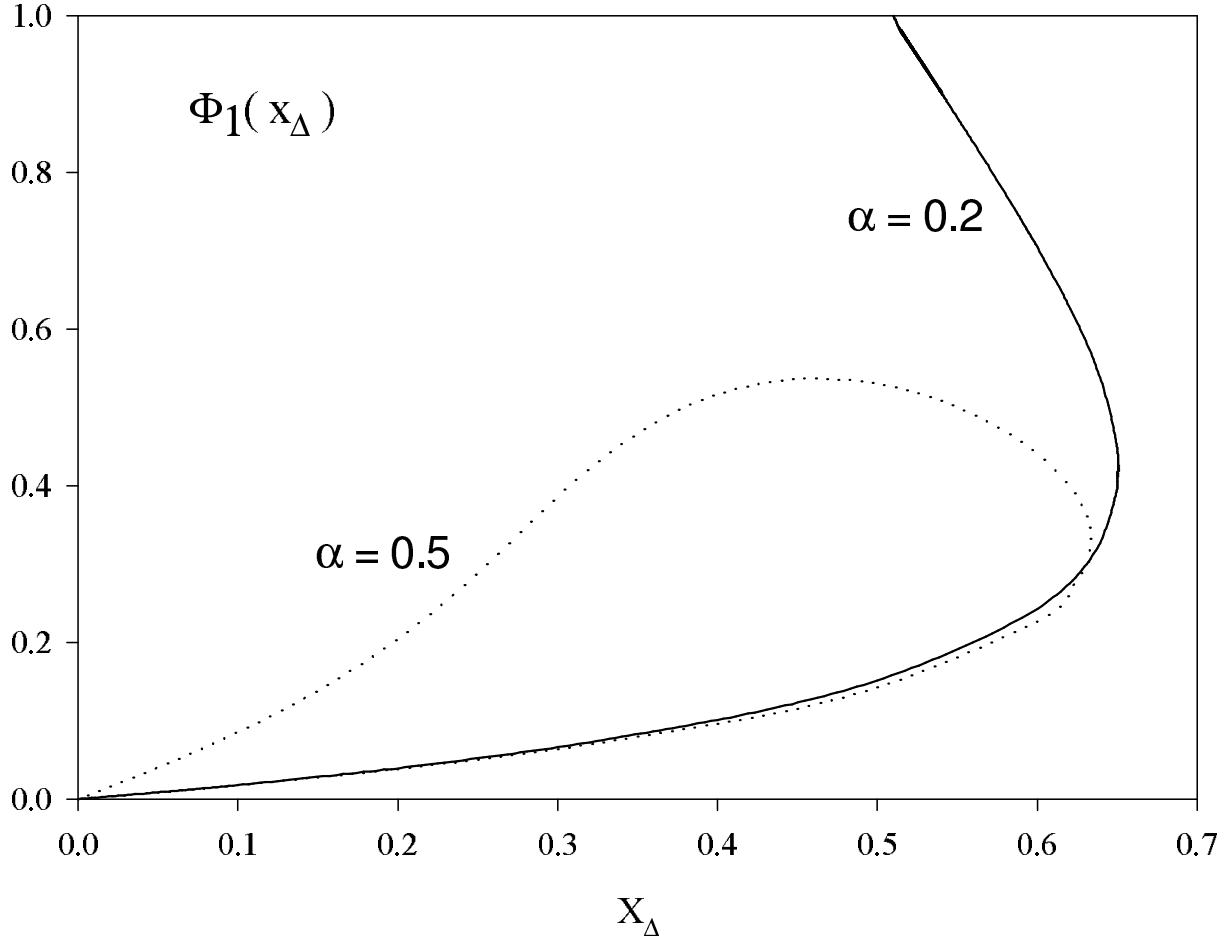


Figure 5. The value of the gauge field function Φ_1 of the uniform black string ($m = 0$; $n = 1$) at the horizon, $\Phi_1(x_\Delta)$, is shown as function of x_Δ for $\alpha = 0.2$ and $\alpha = 0.5$. The lower and upper curves correspond to the 1., respectively 2. branch of solutions.

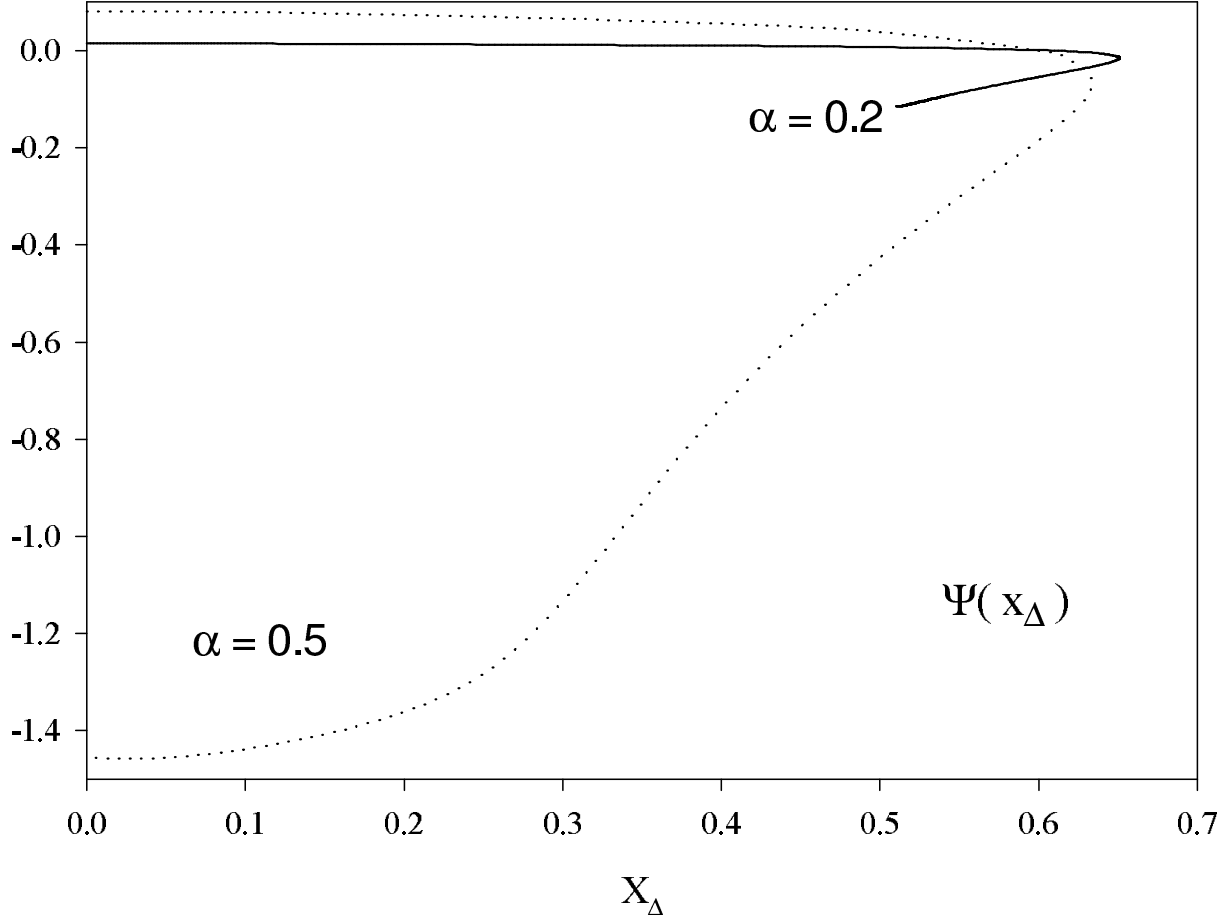


Figure 6. The value of the metric function of the uniform black string ($m = 0$; $n = 1$) at the horizon (x_Δ), is shown as function of x_Δ for $\alpha = 0.2$ and $\alpha = 0.5$. The upper and lower curves correspond to the 1., respectively 2. branch of solutions.

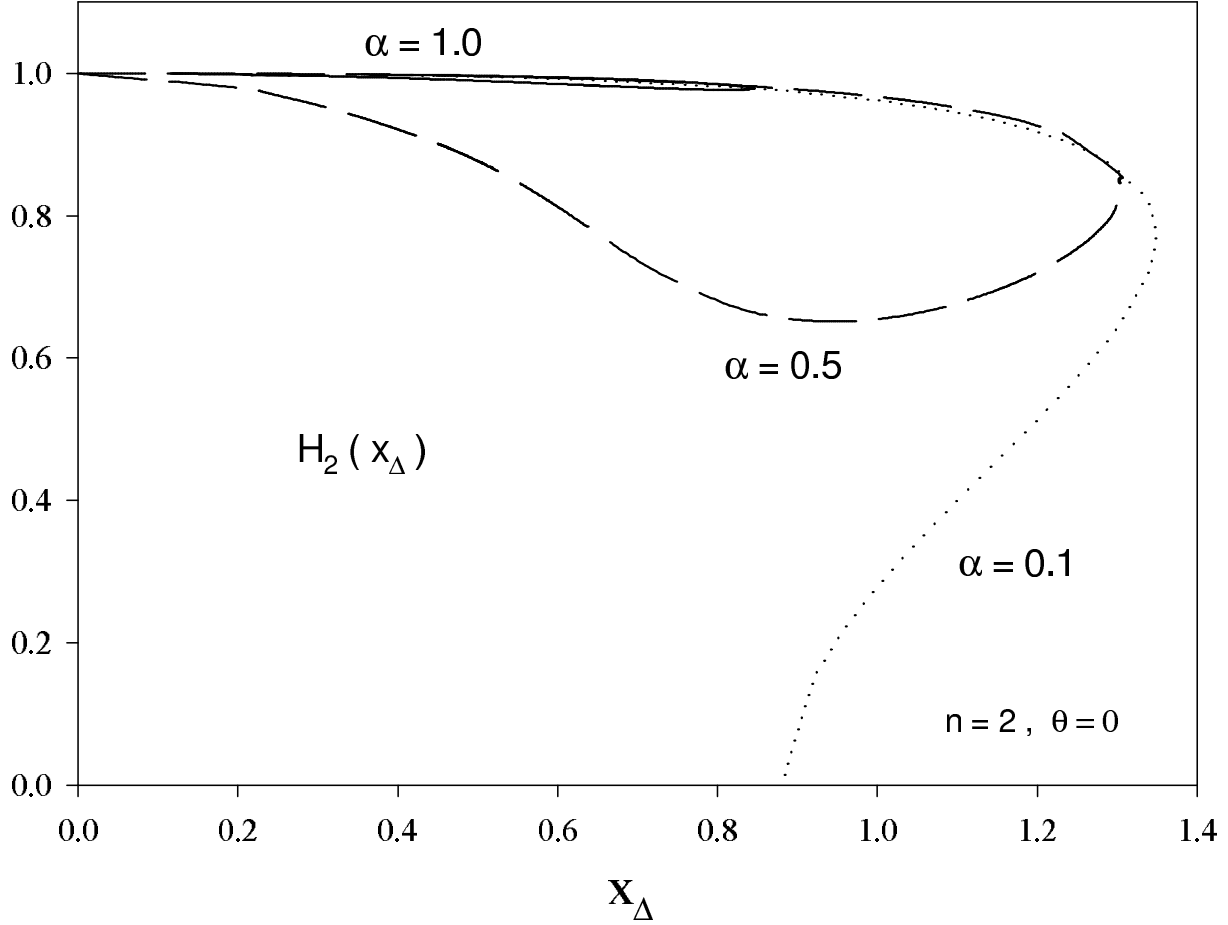


Figure 7. The value of the gauge field function H_2 of the deformed black string ($m = 0$; $n = 2$) at the horizon, $H_2(x_\Delta; \theta = 0)$ is shown as function of x_Δ for $\alpha = 0.1$ and $\alpha = 0.5$. The upper and lower curves correspond to the 1., respectively 2. branch of solutions. Here and in Figures 8, 9 the curves for different θ are essentially equal to those for $\theta = 0$.

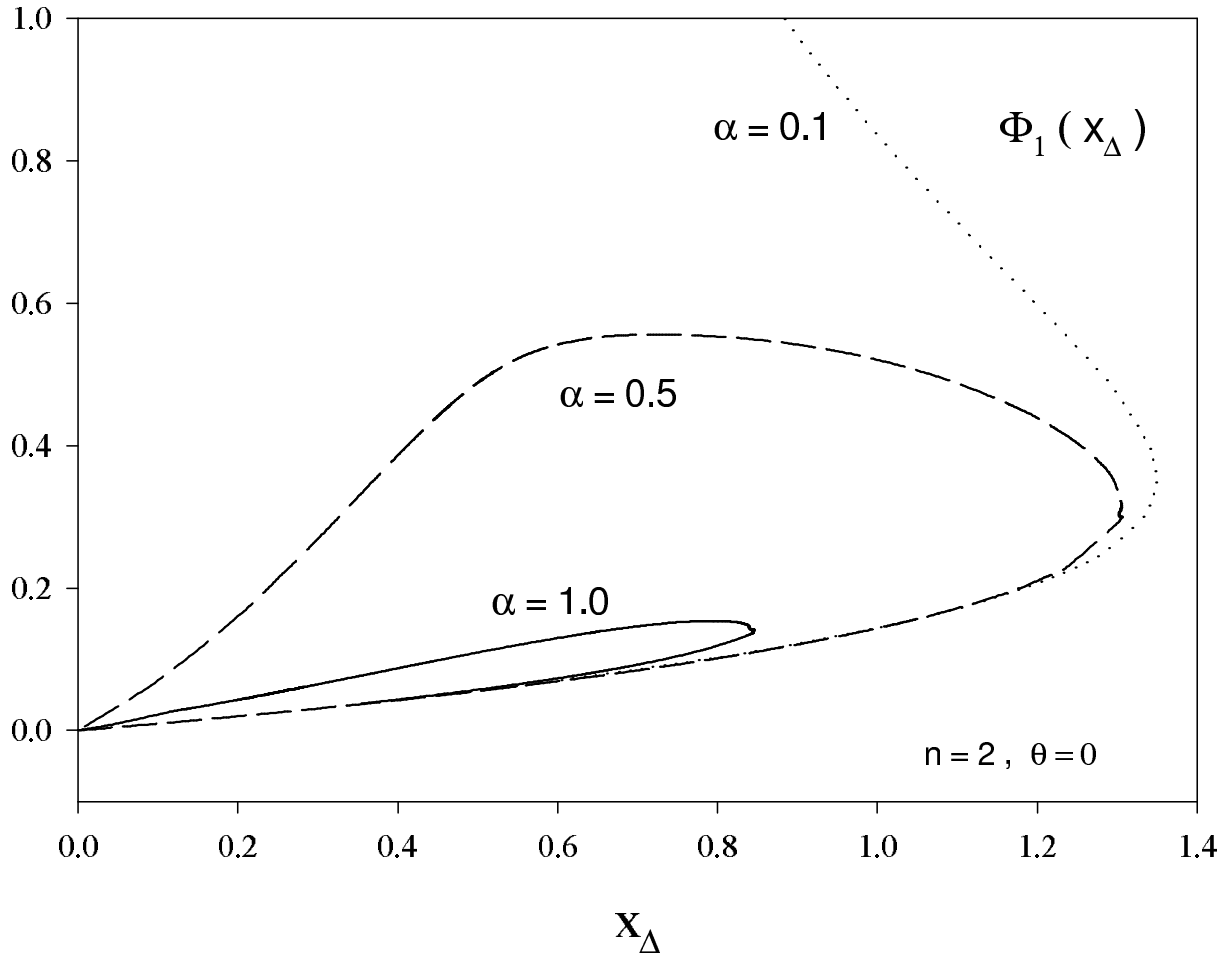


Figure 8. The value of the gauge field function Φ_1 of the deformed black string ($m = 0$; $n = 2$) at the horizon, $\Phi_1(x_\Delta; \theta = 0)$ is shown as function of x_Δ for $\alpha = 0.1$, $\alpha = 0.5$ and $\alpha = 1.0$. The lower and upper curves correspond to the 1., respectively 2. branch of solutions.

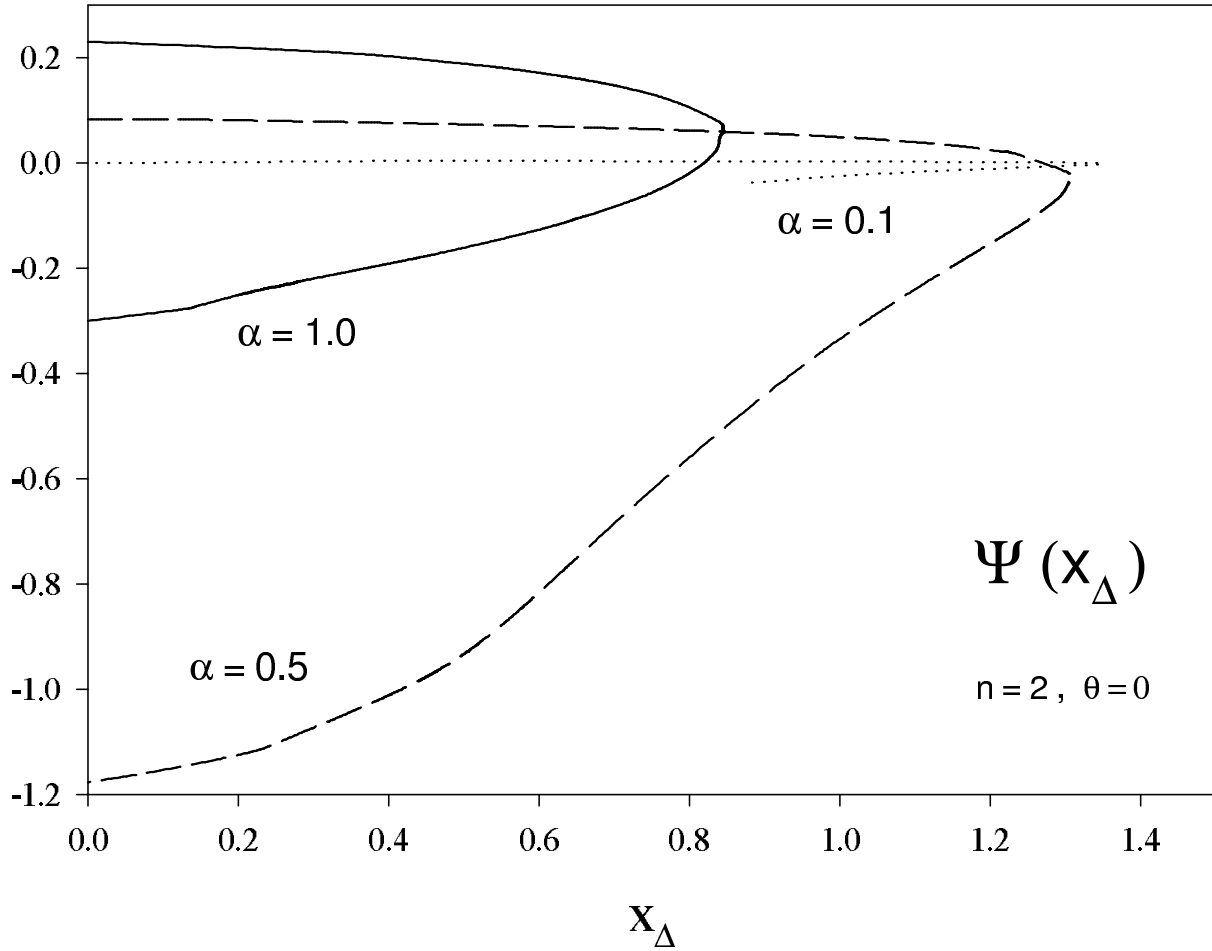


Figure 9. The value of the metric function of the deformed black string ($m = 0$; $n = 2$) at the horizon ($x_{\Delta} = 0$) is shown as function of x_{Δ} for $\alpha = 0.1$, $\alpha = 0.5$ and $\alpha = 1.0$. The upper and lower curves correspond to the 1., respectively 2. branch of solutions.

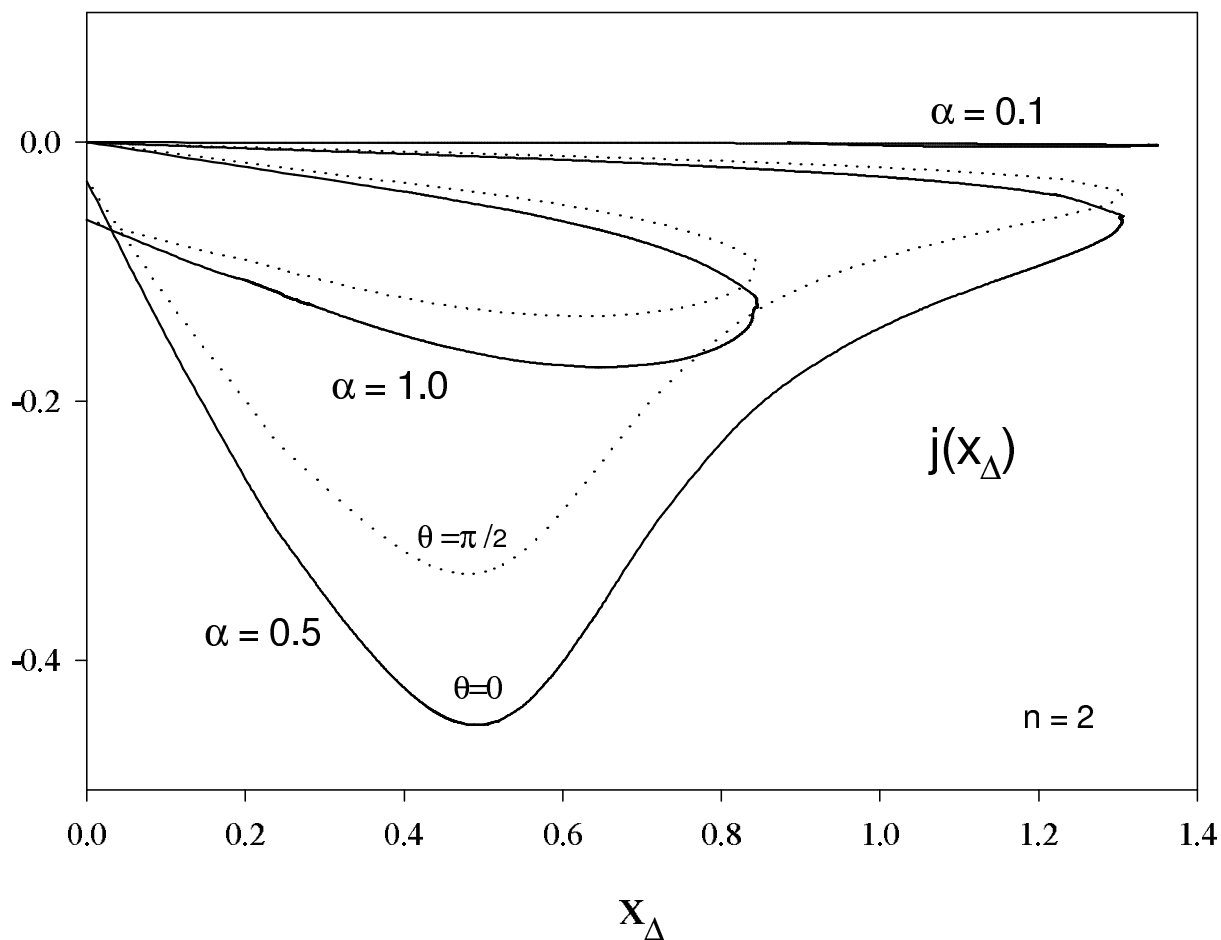


Figure 10. The value of the metric function j used in the Ansatz described in Appendix B of the deformed black string ($m = 0$; $n = 2$) at the horizon, $j(x_\Delta)$ is shown as function of x_Δ for $\alpha = 0.1$, $\alpha = 0.5$ and $\alpha = 1.0$. We show the curves for $\theta = 0$ (solid) and $\theta = \pi/2$ (dotted). The upper and lower curves correspond to the 1., respectively 2. branch of solutions.

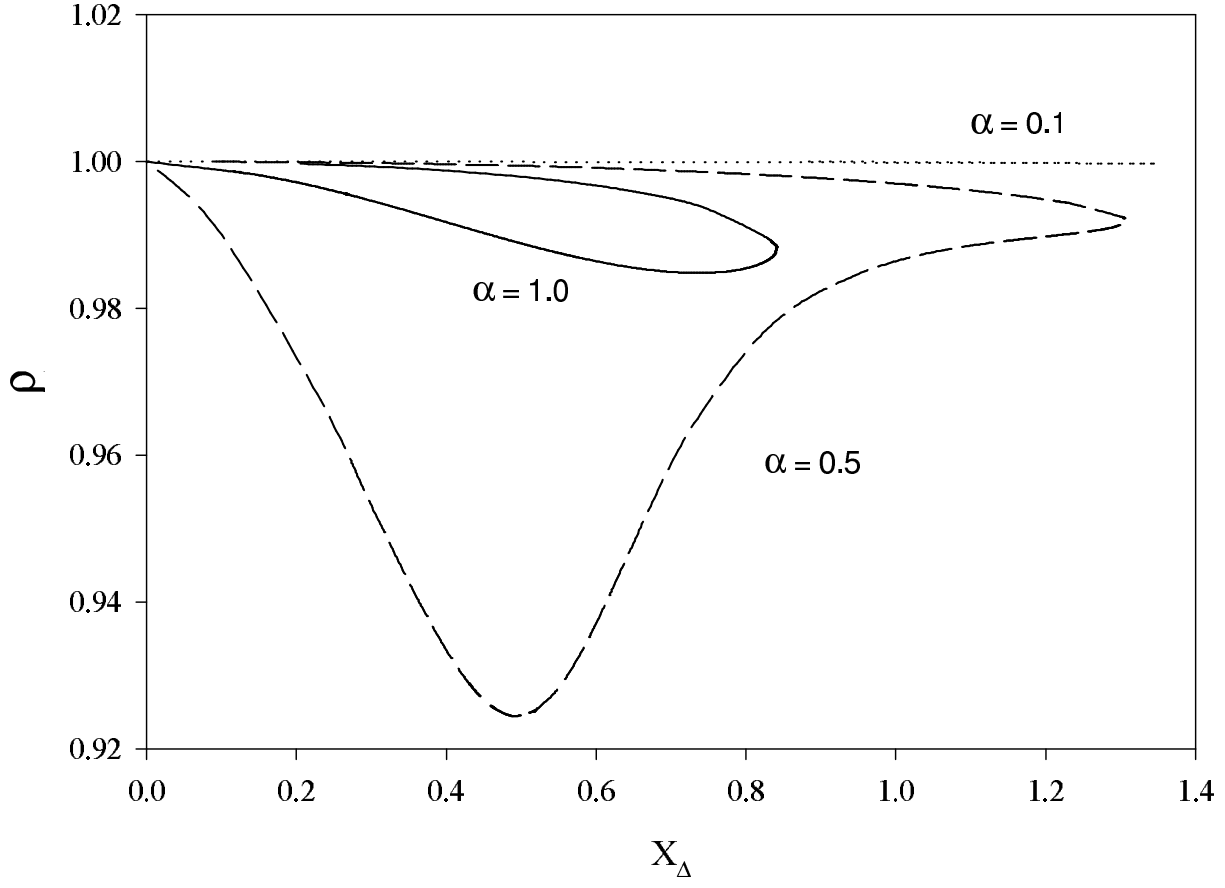


Figure 11. The ratio $\rho = L_e/L_p$ of the horizon circumference along the equator L_e and along the poles L_p is shown for the deformed black strings ($m = 0; n = 2$) as function of the horizon parameter x for $\alpha = 0.1$, $\alpha = 0.5$ and $\alpha = 1.0$. The upper and lower curves correspond to the 1., respectively 2. branch of solutions.

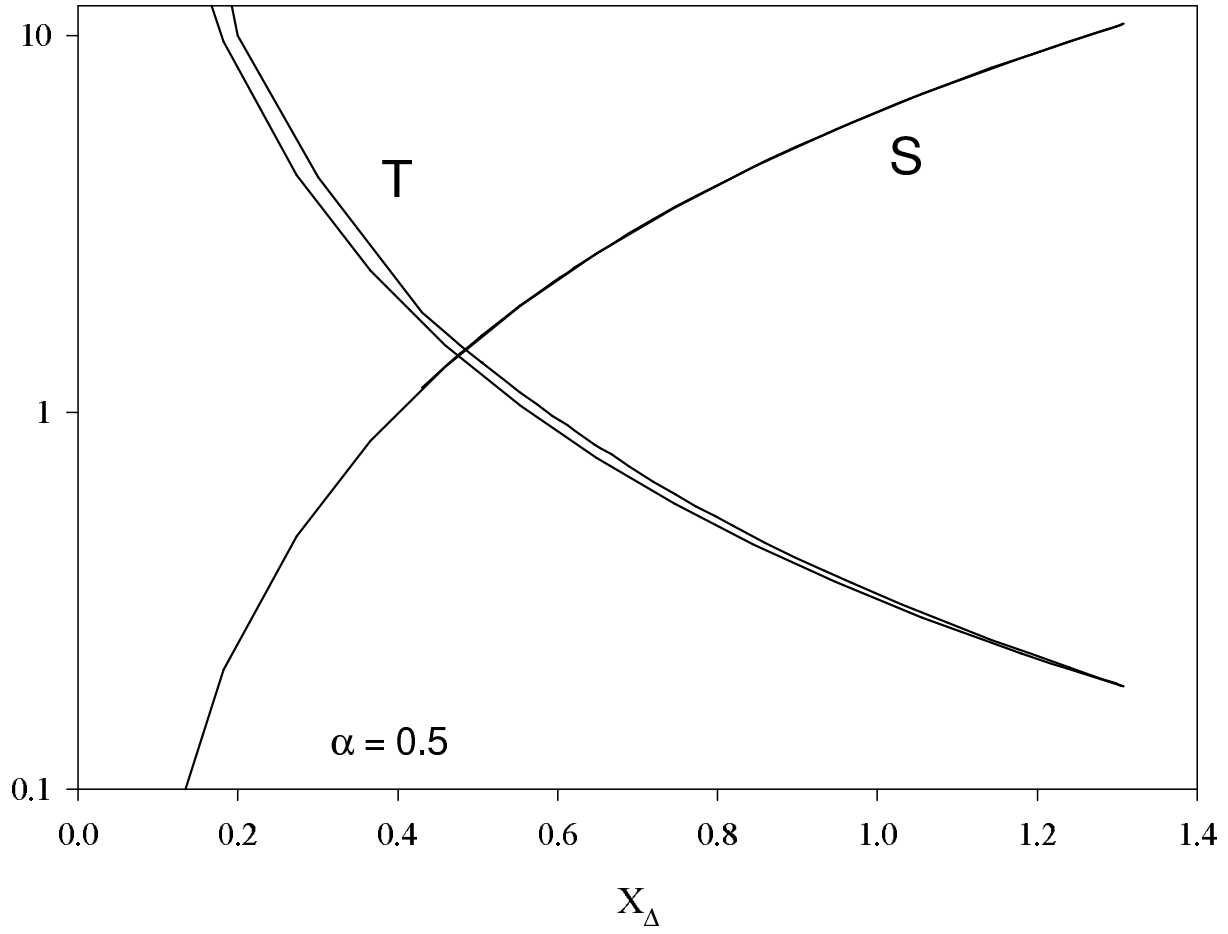


Figure 12. The temperature T and the entropy S of the deformed black strings ($m = 0$; $n = 2$) are shown as functions of x for $\alpha = 0.5$

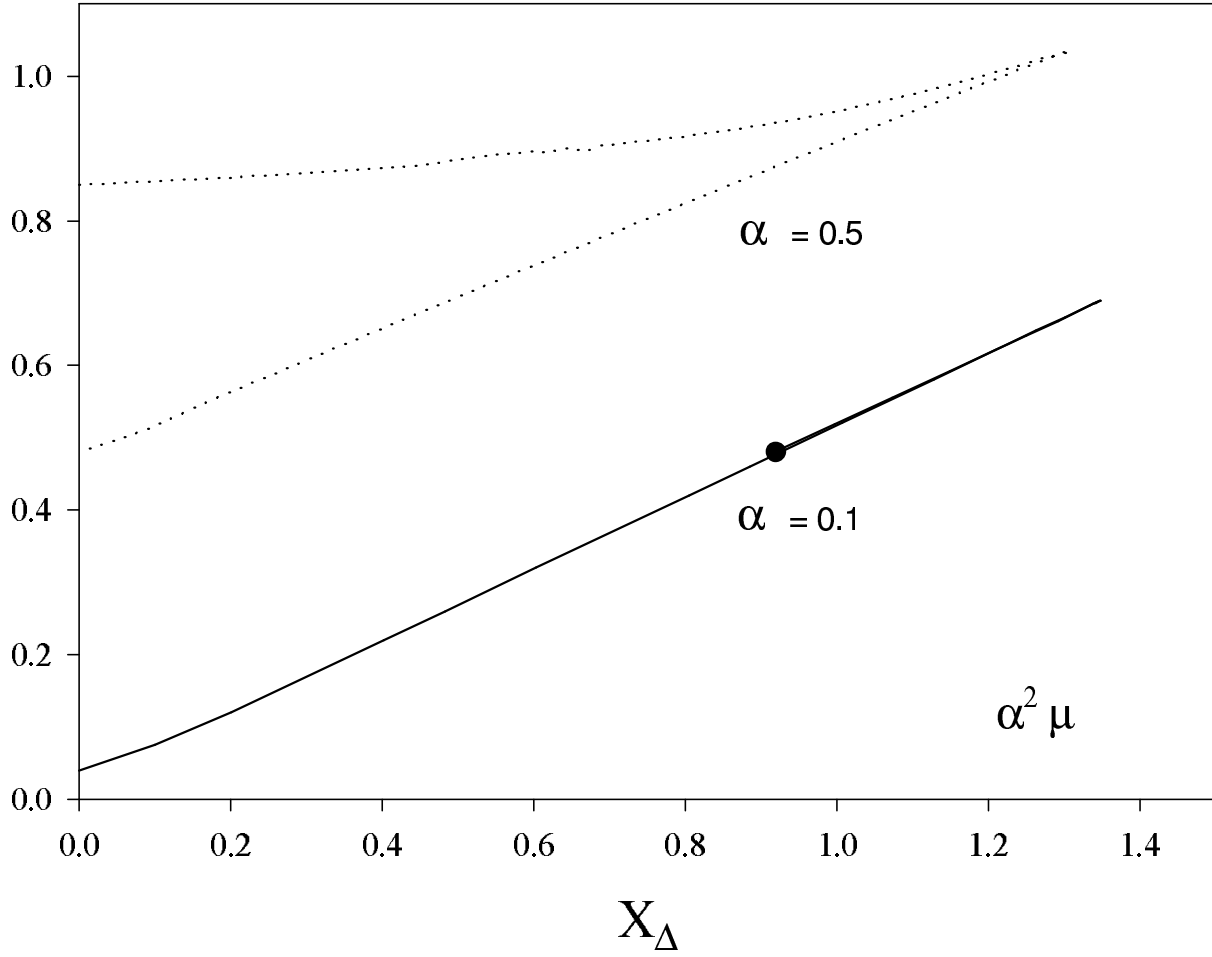


Figure 13. The mass of the ($m = 0$; $n = 2$) deformed black string solutions is shown as function of x for $\alpha = 0.1$ and $\alpha = 0.5$. On the $\alpha = 0.1$ plot, the bullet shows where the second branch stops. The lower and upper curves correspond to the 1., respectively 2. branch of solutions.

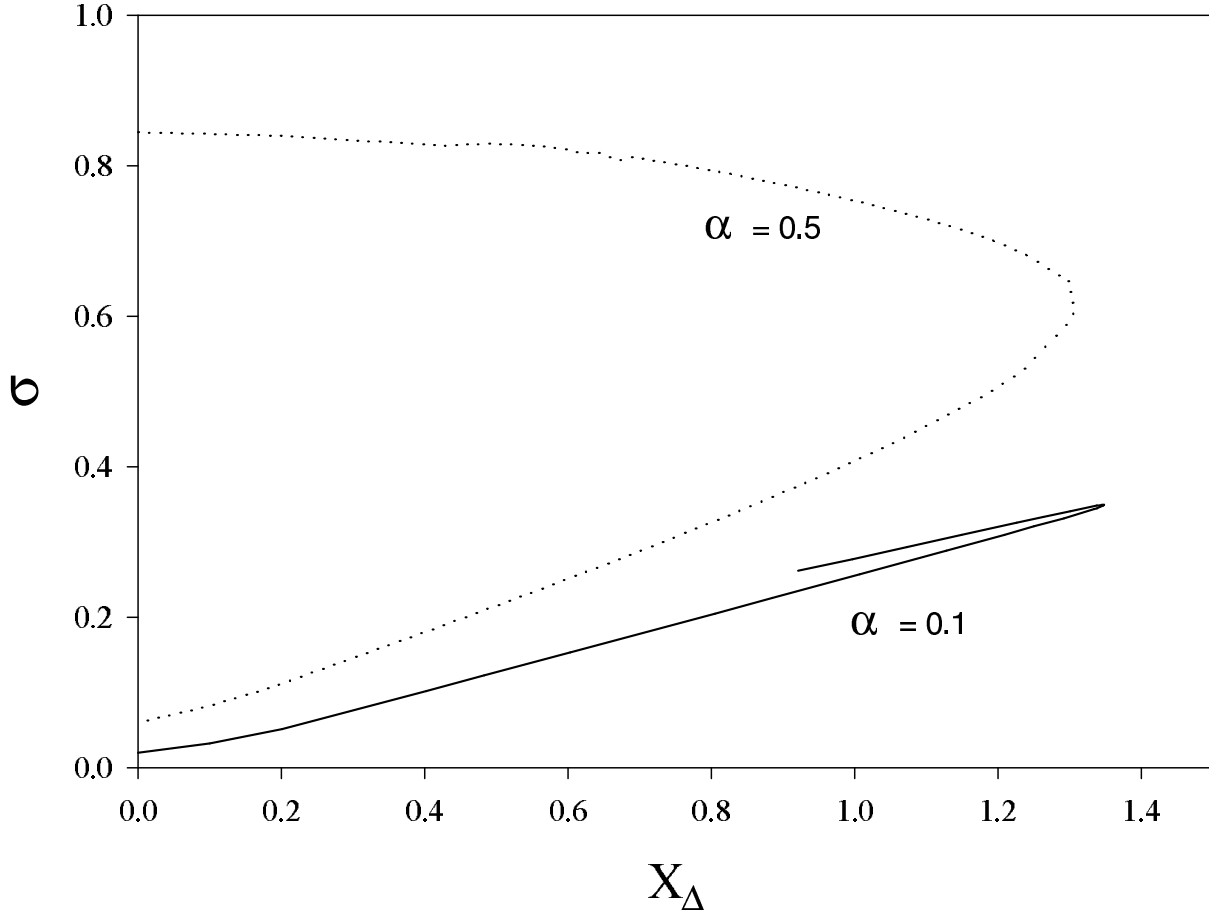


Figure 14. The tension σ of the $(m = 0; n = 2)$ deformed black string solutions is shown as function of x for $\alpha = 0.1$ and $\alpha = 0.5$. The lower and upper curves correspond to the 1., respectively 2. branch of solutions.

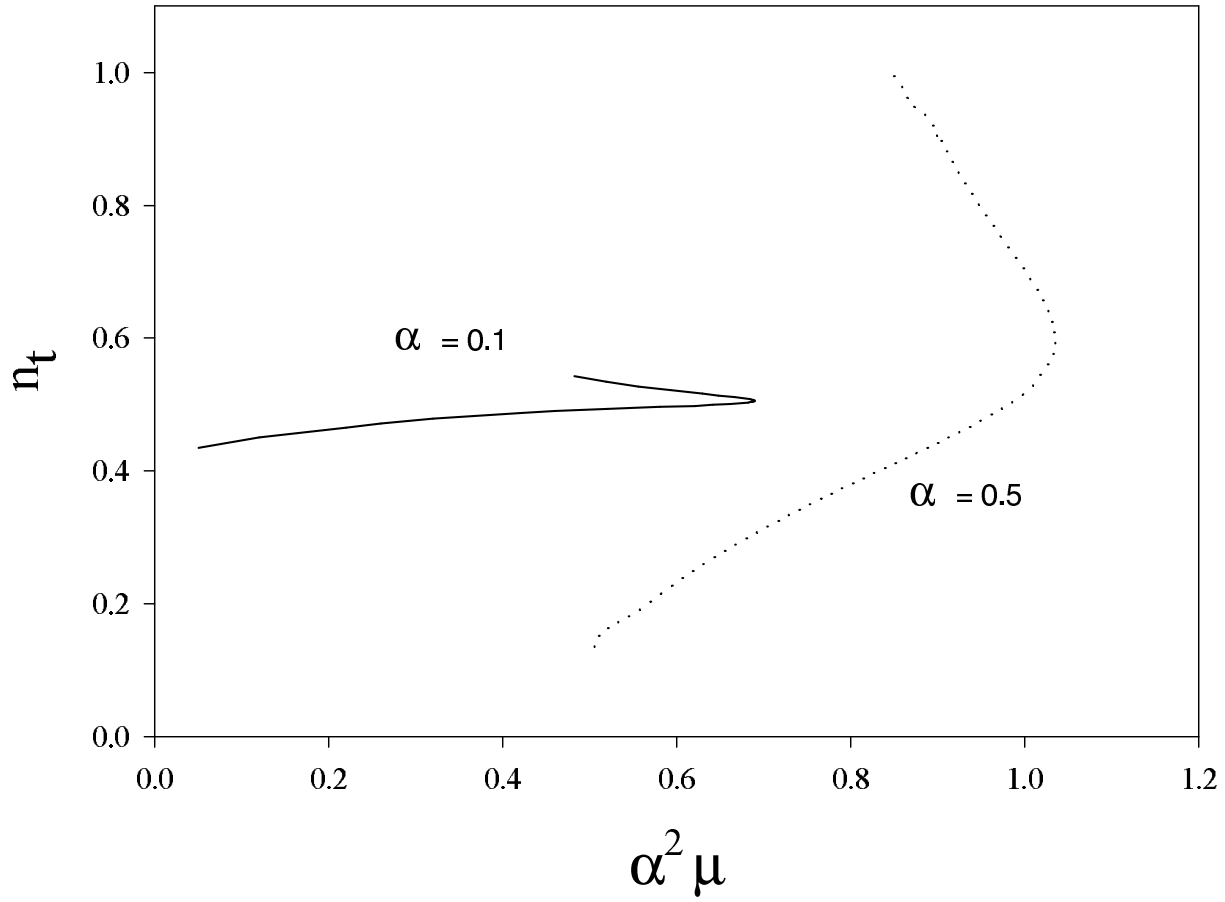


Figure 15. A $(\alpha^2 \mu; n_t)$ diagram is plotted for $(m = 0; n = 2)$ deformed black string solutions and two values of α .

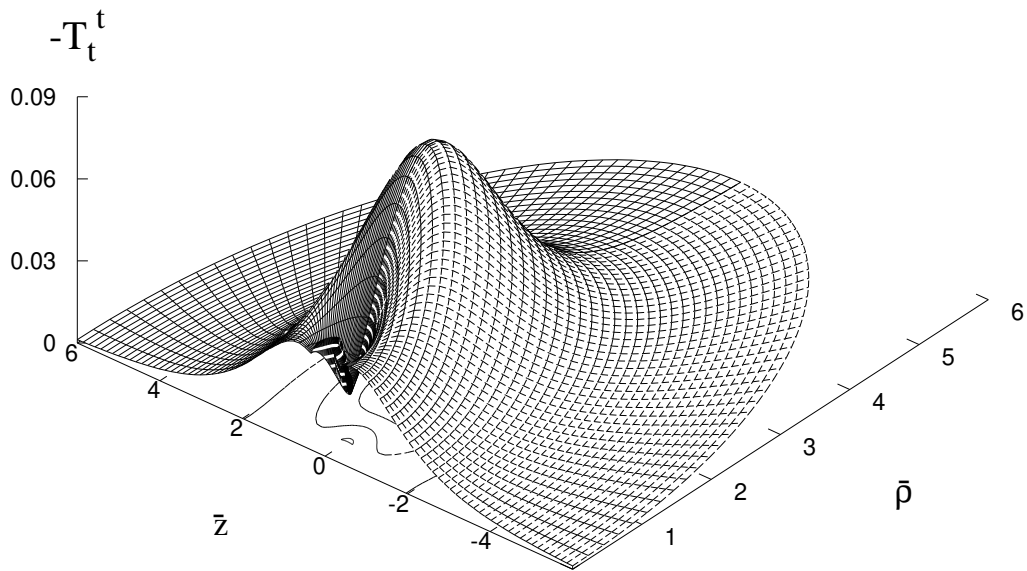


Figure 16. The energy density of the matter fields $-T_t^t$ is shown as a function of the coordinates $\bar{\rho} = r \sin \theta$, $\bar{z} = r \cos \theta$ for a $(m = 0; n = 2)$ deformed black string solution with $\alpha = 0.5$; $\beta = 0.2$.

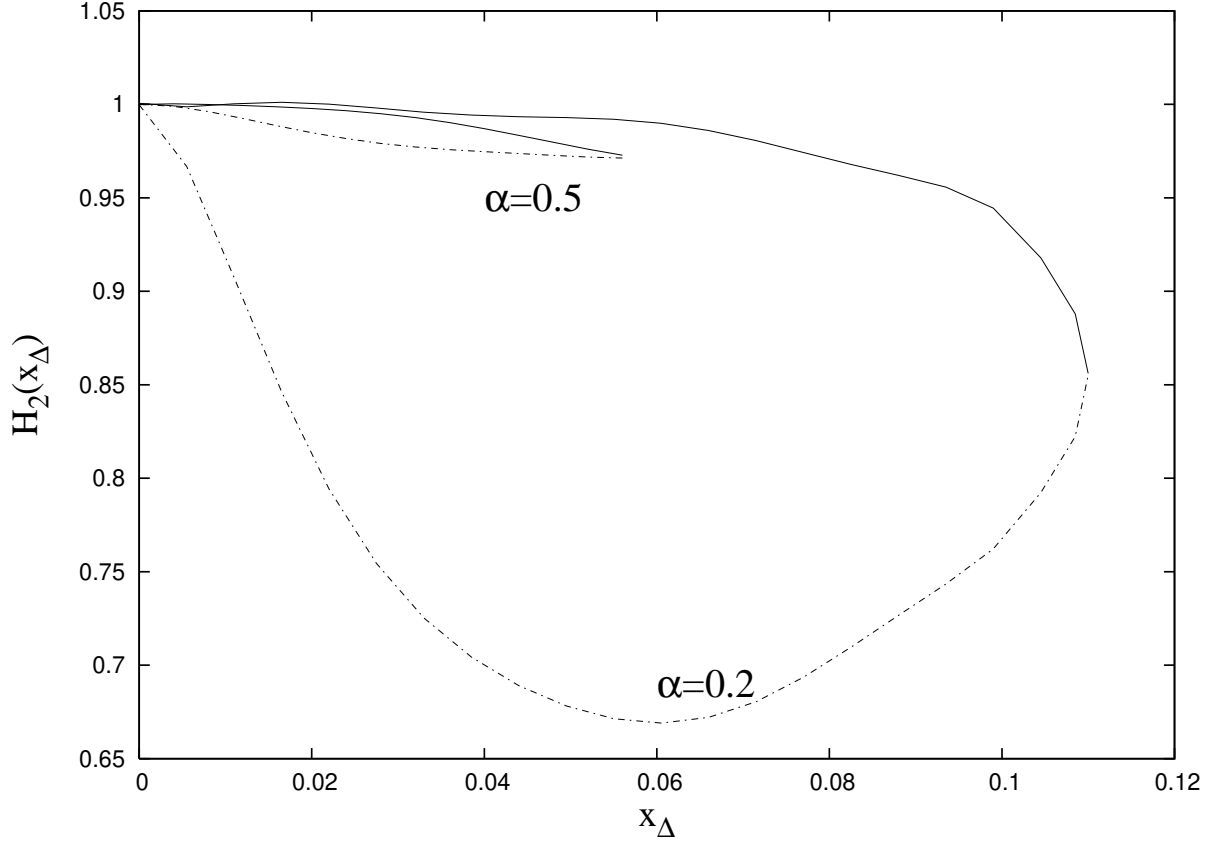


Figure 17. The value of the gauge field function H_2 at the horizon, $H_2(x_\Delta; \epsilon = 0)$ is shown as function of x_Δ for $(m = 1; n = 1)$ black string solutions with $\alpha = 0.2$ and $\alpha = 0.5$. Here and in Figures 18-25, the dotted line denotes the higher branch solution, the continuous line corresponding to the fundamental branch.

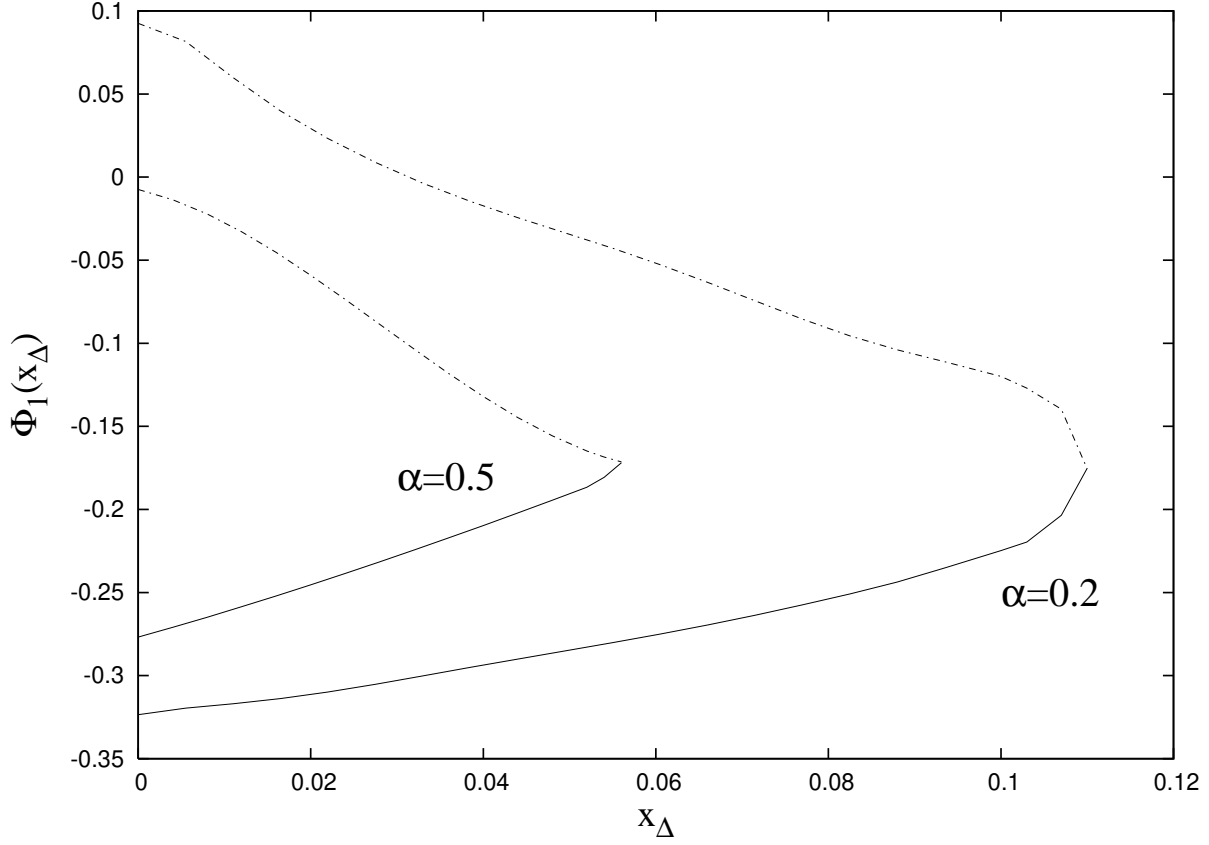


Figure 18. The value of the gauge field function Φ_1 at the horizon, $\Phi_1(x_\Delta; \alpha=0)$ is shown as function of x_Δ for $(m=1; n=1)$ black string solutions with $\alpha=0.2$ and $\alpha=0.5$.

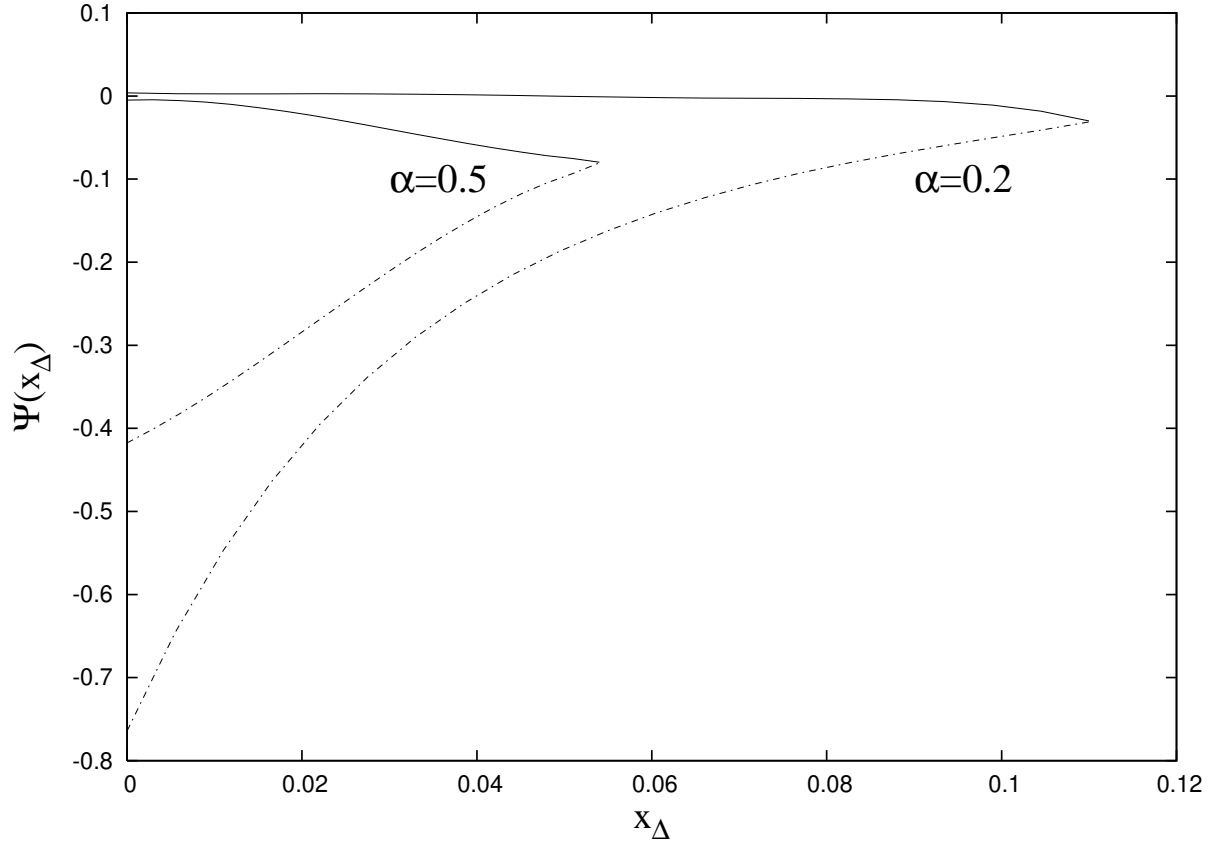


Figure 19. The value of the metric function at the horizon ($x_\Delta = 0$) is shown as function of x_Δ for $(m = 1; n = 1)$ black string solutions with $\alpha = 0.2$ and $\alpha = 0.5$.

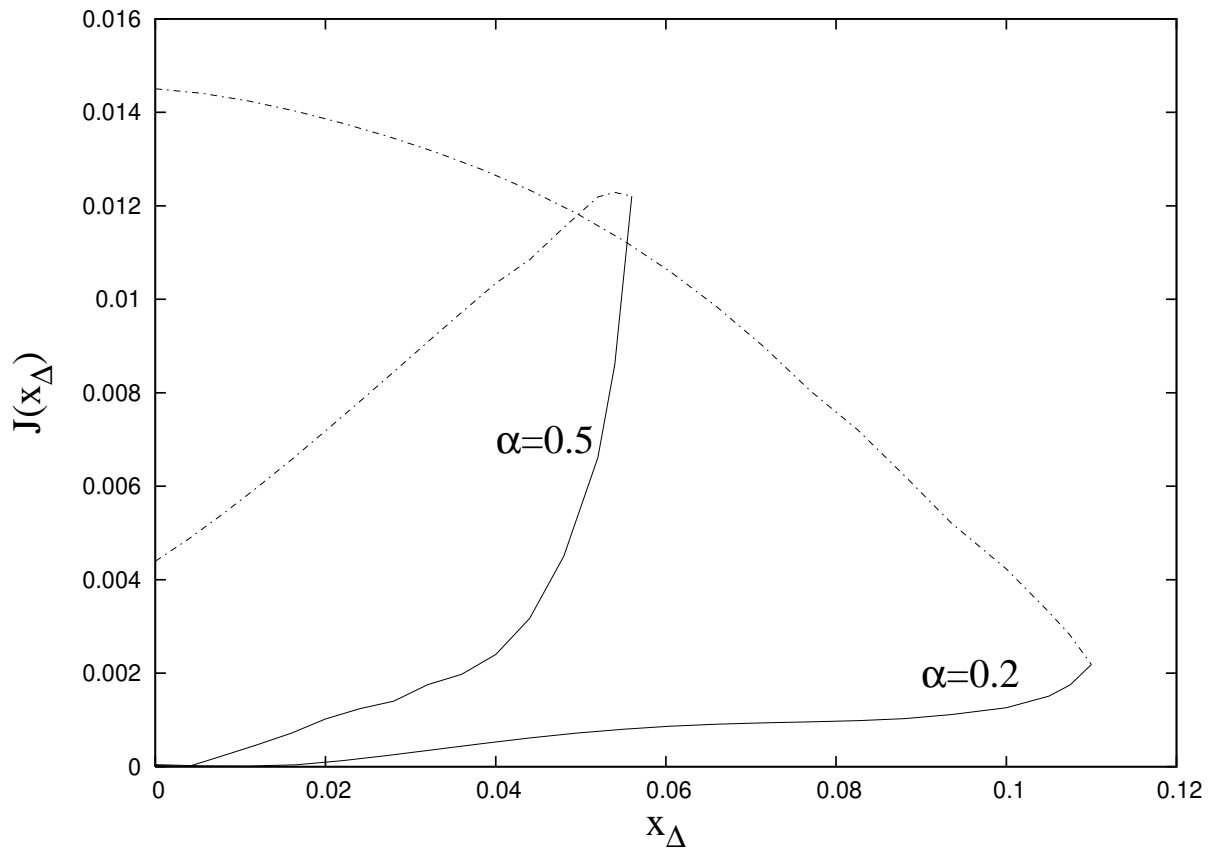


Figure 20. The value of the metric function J at the horizon, $J(x_\Delta; \alpha=2)$ is shown as function of x_Δ for $(m=1; n=1)$ black string solutions with $\alpha=0.2$ and $\alpha=0.5$.

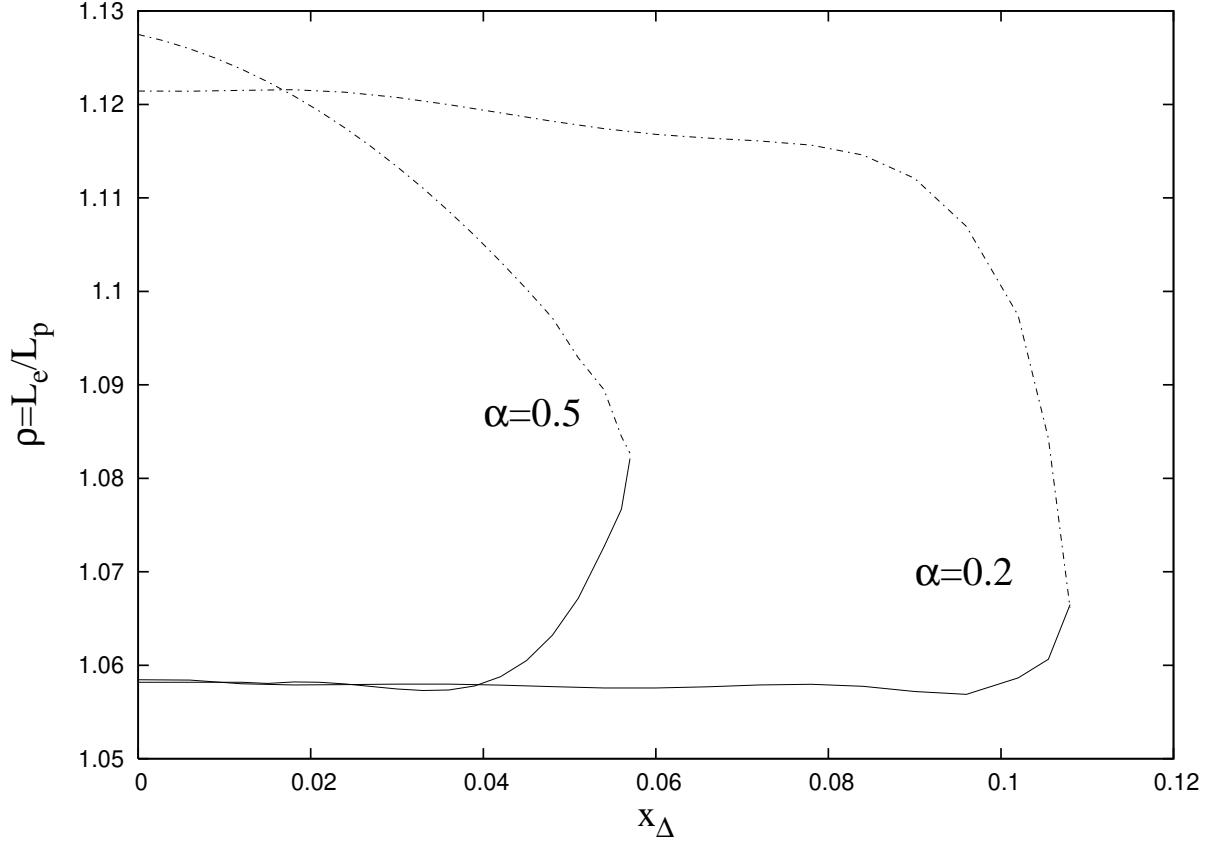


Figure 21. The ratio $\rho = L_e/L_p$ of the horizon circumference along the equator L_e and along the poles L_p is shown for $(m = 1; n = 1)$ black string solutions as function of the horizon parameter x_{Δ} for $\alpha = 0.2$ and $\alpha = 0.5$.

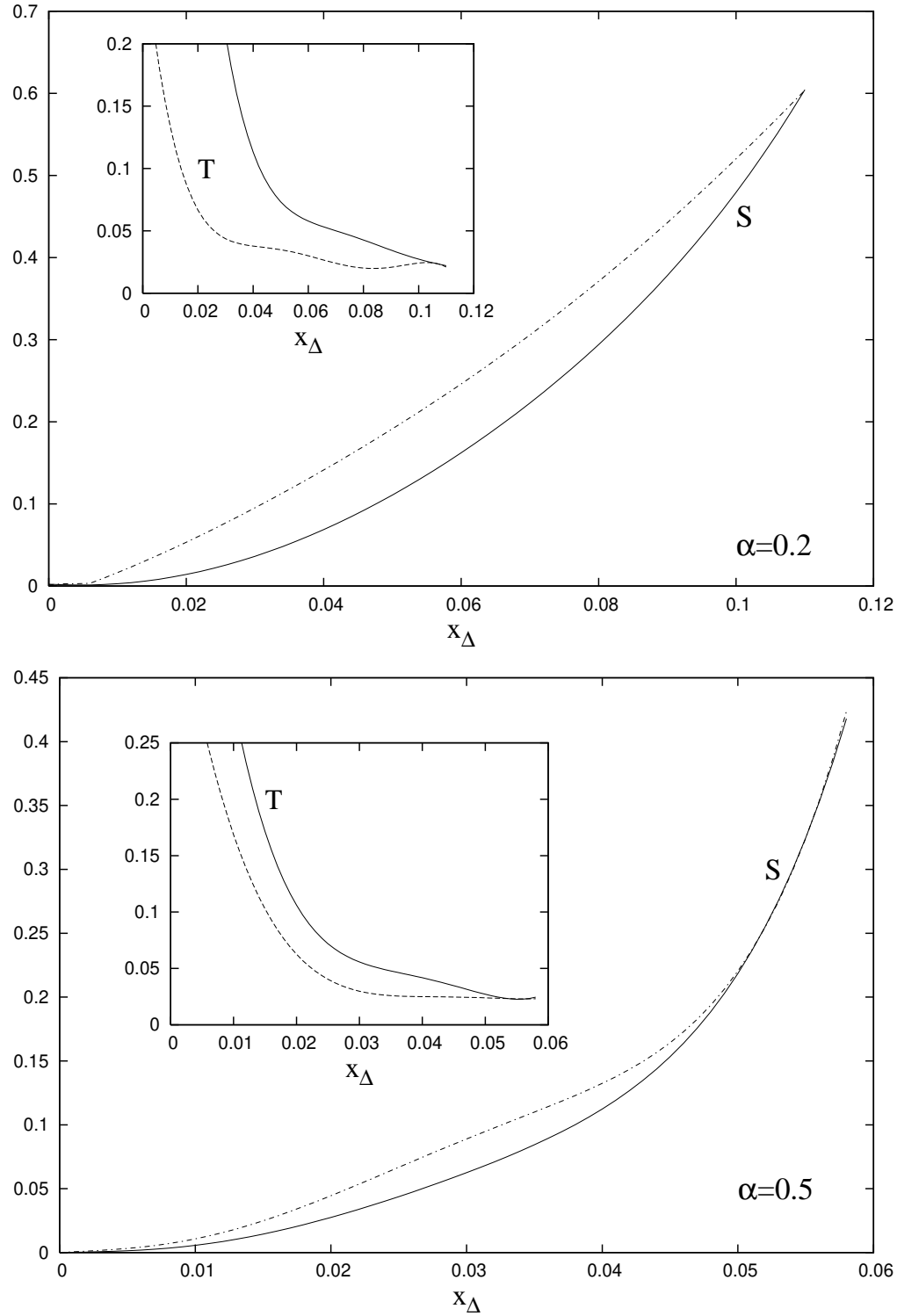


Figure 22. The temperature T and the entropy S are shown as functions of x for $(m = 1; n = 1)$ black string solutions with $\alpha = 0.2$ and $\alpha = 0.5$.

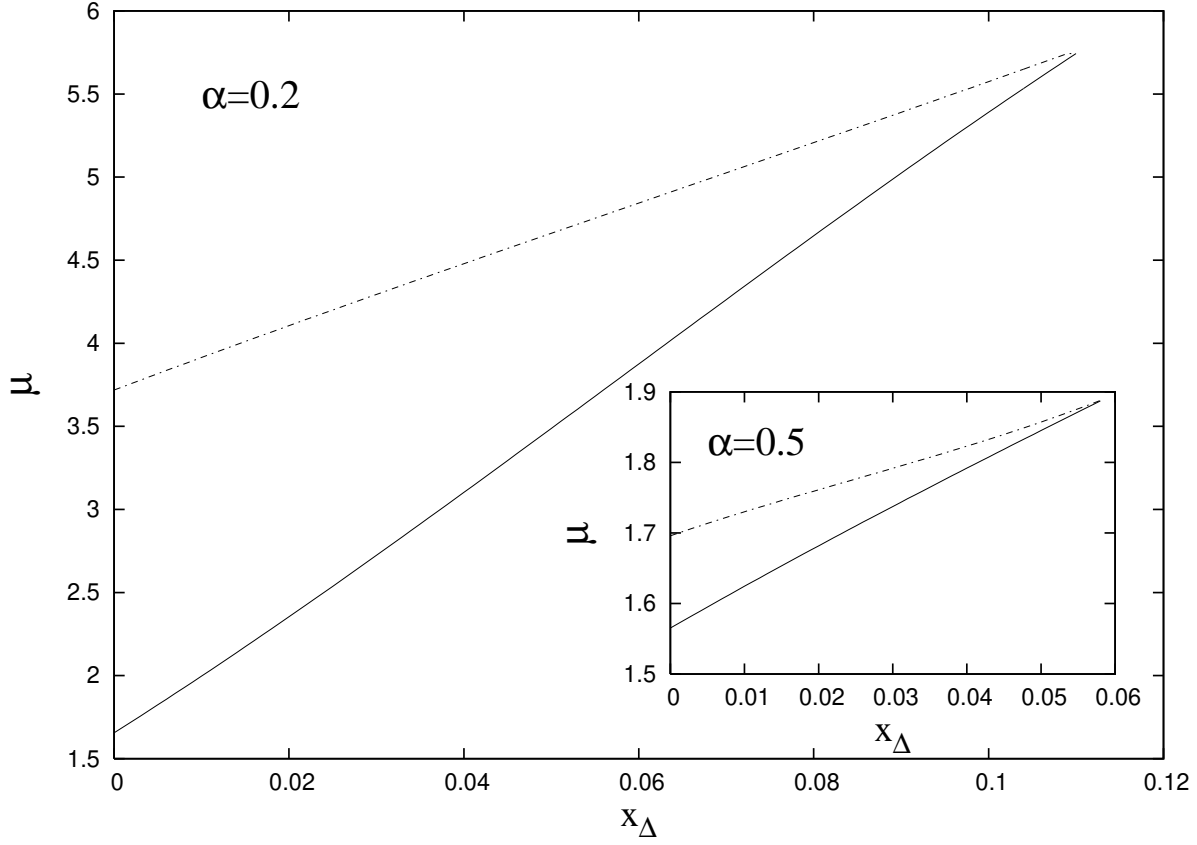


Figure 23. The mass of the $(m = 1; n = 1)$ black string solutions is shown as function of x for $\alpha = 0.2$ and $\alpha = 0.5$.

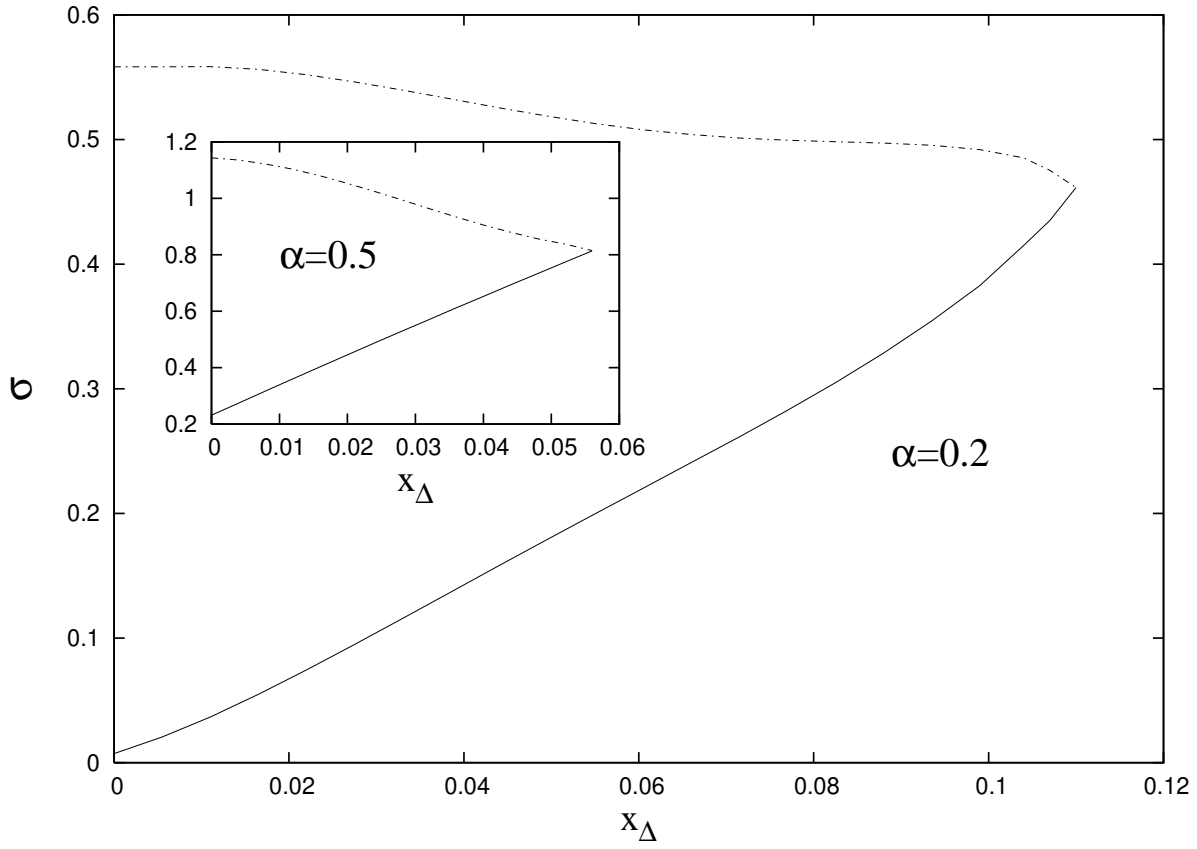


Figure 24. The tension of the $(m = 1; n = 1)$ black string solutions is shown as function of x for $\alpha = 0.2$ and $\alpha = 0.5$.

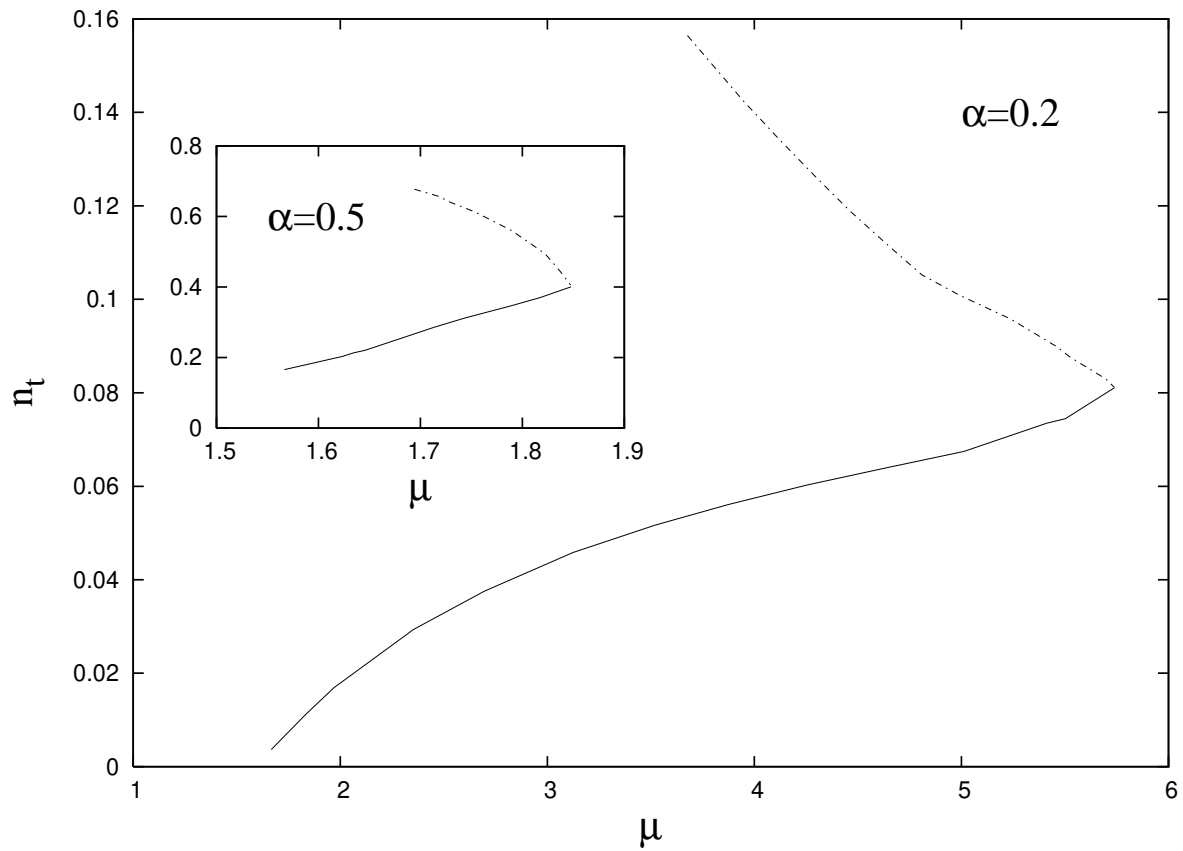


Figure 25. A $(\mu; n_t)$ diagram is plotted for $(m = 1; n = 1)$ black string solutions and two values of α .

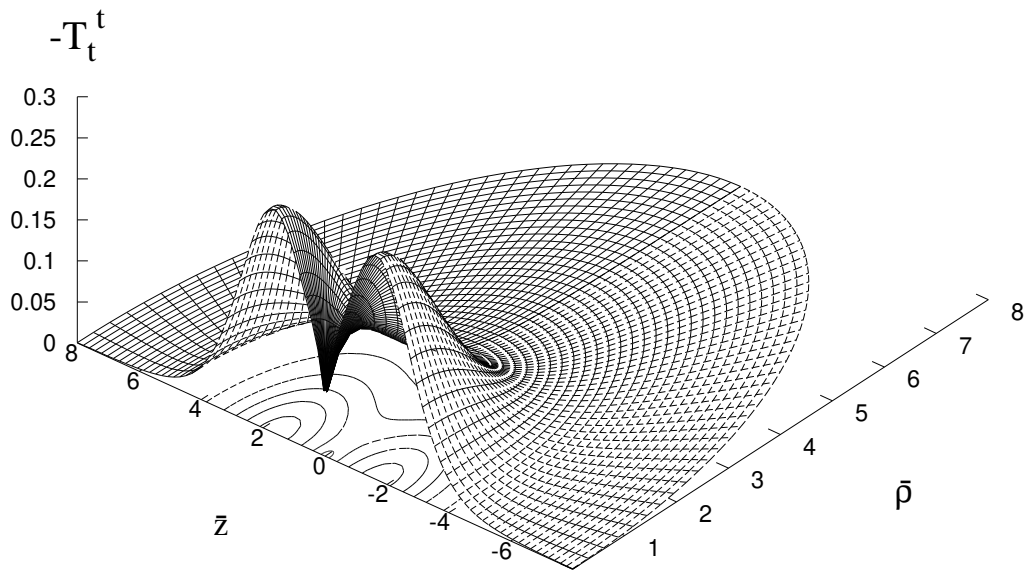


Figure 26. The energy density of the matter fields $\mathcal{E} = -T_t^t$ is shown as a function of the coordinates $\bar{\rho} = r \sin \theta$, $\bar{z} = r \cos \theta$ for a $(m = 1; n = 1)$ lower branch black string solution with $\alpha = 0.2$ & $\beta = 0.04$.